

Article

Synthesis of 3,5-Bis(trifluoromethyl)phenyl-Substituted Pyrazole Derivatives as Potent Growth Inhibitors of Drug-Resistant Bacteria

Ibrahim S. Alkhaibari ¹, Hansa Raj KC ¹, Subrata Roy ¹, Mohd. K. Abu-gazleh ¹ , David F. Gilmore ² 
and Mohammad A. Alam ^{1,*} 

¹ Department of Chemistry and Physics, The College of Sciences and Mathematics, Arkansas State University, Jonesboro, AR 72401, USA; ibrahimsaleh.s@hotmail.com (I.S.A.); hansa.kc@smail.astate.edu (H.R.K.); subrata.roy@smail.astate.edu (S.R.); mohdkota.abugazle@smail.astate.edu (M.K.A.-g.)

² Department of Biological Sciences, The College of Sciences and Mathematics, Arkansas State University, Jonesboro, AR 72401, USA; dgilmore@astate.edu

* Correspondence: malam@astate.edu

Abstract: Enterococci and methicillin-resistant *S. aureus* (MRSA) are among the menacing bacterial pathogens. Novel antibiotics are urgently needed to tackle these antibiotic-resistant bacterial infections. This article reports the design, synthesis, and antimicrobial studies of 30 novel pyrazole derivatives. Most of the synthesized compounds are potent growth inhibitors of planktonic Gram-positive bacteria with minimum inhibitory concentration (MIC) values as low as 0.25 µg/mL. Further studies led to the discovery of several lead compounds, which are bactericidal and potent against MRSA persisters. Compounds **11**, **28**, and **29** are potent against *S. aureus* biofilms with minimum biofilm eradication concentration (MBEC) values as low as 1 µg/mL.

Keywords: pyrazole; aniline; *Staphylococcus aureus*; *Enterococcus faecium*; MRSA; *Enterococcus faecalis*; VRE



Citation: Alkhaibari, I.S.; KC, H.R.; Roy, S.; Abu-gazleh, M.K.; Gilmore, D.F.; Alam, M.A. Synthesis of 3,5-Bis(trifluoromethyl)phenyl-Substituted Pyrazole Derivatives as Potent Growth Inhibitors of Drug-Resistant Bacteria. *Molecules* **2021**, *26*, 5083. <https://doi.org/10.3390/molecules26165083>

Academic Editor: Brullo Chiara

Received: 4 August 2021

Accepted: 19 August 2021

Published: 22 August 2021

Publisher's Note: MDPI stays neutral with regard to jurisdictional claims in published maps and institutional affiliations.



Copyright: © 2021 by the authors. Licensee MDPI, Basel, Switzerland. This article is an open access article distributed under the terms and conditions of the Creative Commons Attribution (CC BY) license (<https://creativecommons.org/licenses/by/4.0/>).

1. Introduction

Drug-resistant ESKAPE (*Enterococcus faecium*, *Staphylococcus aureus*, *Klebsiella pneumoniae*, *Acinetobacter baumannii*, *Pseudomonas aeruginosa*, and *Enterobacter* species) pathogens cause a majority of nosocomial infections all over the world. These multidrug-resistant bacteria have reduced treatment options, increased hospital stays and treatment costs, and amplified the death rate of infected patients [1]. *E. faecium* causes a variety of problems, including urinary tract, intra-abdominal, pelvic, and soft tissue infections, bacteremia, and endocarditis [2]. Approximately 30% of all healthcare-associated enterococcal infections are caused by *E. faecalis* and *E. faecium*, which are vancomycin-resistant (VRE), and these resistant strains are increasingly becoming resistant to other antibiotics. VRE is the most common cause of central line-associated bloodstream infections [3]. Furthermore, enterococcal biofilms cause 25% of all catheter-associated urinary tract infections [4]. Alcohol tolerance (ethanol and isopropanol) of clinical isolates of *E. faecium* has increased over the years, and isolates obtained after 2010 are 10-fold more tolerant to killing by alcohol than were older isolates [5]. *S. aureus* infections are caused by different strains, including methicillin-sensitive *S. aureus* (MSSA), methicillin-resistant *S. aureus* (MRSA), vancomycin-intermediate *S. aureus* (VISA), and vancomycin-resistant *S. aureus* (VRSA). Infections by MRSA are the most problematic, but any *S. aureus* infection can become serious [6]. MRSA causes ten-fold more infections than all multidrug-resistant (MDR) Gram-negative bacteria combined [7]. MRSA has emerged as one of the most menacing pathogens of humans, and this pathogen currently bypasses HIV in terms of fatality rate [8]. Hospitals are the hotbeds for highly drug-resistant pathogens, such as MRSA, increasing the risk of hospitalization kills instead of cures [9].

1*H*-Pyrazole (1,2-diazole) is a five-membered heterocycle, and its derivatives are known for a wide spectrum of biological activities [10]. It is found as the core structure of several leading drugs, such as celecoxib, a potent anti-inflammatory medicine [11]; tepoxalin, a nonsteroidal anti-inflammatory agent for veterinary use [10]; the anti-obesity drug, rimonabant [12]; the analgesic difenamizole [13]; and several other therapeutic agents. A number of drugs containing pyrazole nuclei may be due to its decreased susceptibility to oxidative degradation metabolism compared to other five-membered heterocycles [14]. Pyrazole derivatives have been reported as antimicrobial agents in several publications [15–17]. Although pyrazole derivatives as anti-MRSA agents have been reported by us [18–22] and others [23,24], pyrazole derivatives with anti-Acinetobacterial activity had not been reported until our recent papers [18–22].

The trifluoromethyl ($-CF_3$) group strategically placed on a phenyl ring is known to improve the pharmacodynamics and pharmacokinetic properties of the resulting compounds [25]. A number of widely used drugs, such as dutasteride [26], hydroxyflutamide [27], and cinacalcet [28], contain the trifluoromethyl substituted phenyl moiety (Figure 1). We have found the trifluoromethyl substituted phenyl groups as potent growth inhibitors of different bacterial strains, including MRSA [22,29]. Based on the significance of the trifluoromethyl group in drug discovery, herein, we report the synthesis and antimicrobial activities of 3,5-bis(trifluoromethyl)phenyl substituted pyrazole derivatives as potent antimicrobial agents.

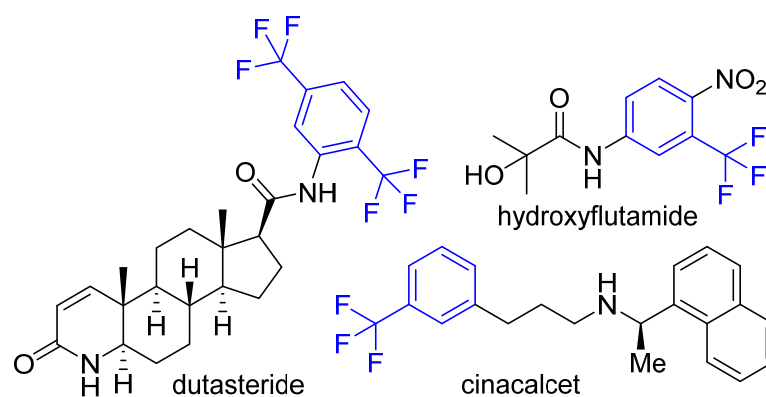


Figure 1. Representative examples of trifluoromethyl phenyl-containing approved drugs.

2. Results and Discussion

The designed compounds were synthesized by the reaction of 3',5'-bis(trifluoromethyl)acetophenone (I) with 4-hydrazinobenzoic acid (II) to form the hydrazone intermediate, which on reaction with the Vilsmeier-Haack reagent formed the pyrazole aldehyde (III) [21,29–31]. This aldehyde intermediate (III) was synthesized on a 10 g scale, and the pure product was obtained simply by filtration and washing with water. Reductive amination of the aldehyde (III) with different anilines ($R-NH_2$) formed the target compounds (1–30) in a very good average yield (Table 1). The synthetic method is very robust as different substituents on the aniline moiety did not affect the yield and purity of the products.

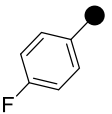
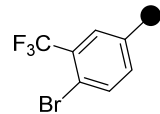
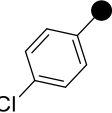
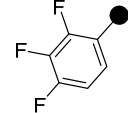
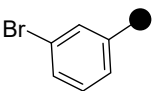
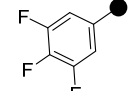
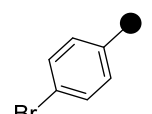
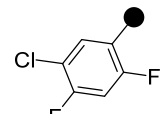
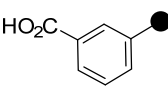
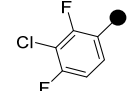
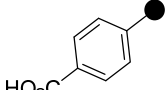
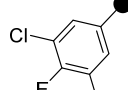
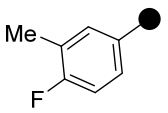
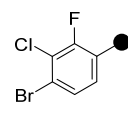
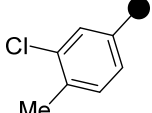
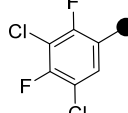
All the synthesized compounds were tested for their activity against Gram-positive and Gram-negative bacteria. These compounds showed broad activity against Gram-positive strains, but no activity against the Gram-negative strains (Table 2). The phenyl-substituted derivative (1) showed moderate activity against the tested bacteria with minimum inhibitory concentration (MIC) values as low as 2 $\mu\text{g}/\text{mL}$. Alkyl substitution on the phenyl ring of the aniline moiety increased the activity of the resultant compounds (2 and 3). 4-Isopropyl aniline derivative (2) inhibited the growth of *S. aureus* strains with MIC values in the range of 1 to 2 $\mu\text{g}/\text{mL}$. Similar potency was observed against *Staphylococcus epidermidis*, enterococci, and *Bacillus subtilis* strains. Methoxy substituent decreased the potency of the product (4) significantly. Activities of the compounds so

far indicated that hydrophobic substituents on the phenyl ring increased the activity of the compounds. The phenoxy-substituted derivative was found to be a potent antimicrobial compound with MIC values of 1 $\mu\text{g}/\text{mL}$ against several bacterial strains. The methyl sulfide attached compound (6) showed activity with MIC values in the range of 1 to 4 $\mu\text{g}/\text{mL}$. Fluorine substituted compounds (7 and 8) were good bacterial growth inhibitors. 3-Fluoro derivative (7) was found to be slightly less potent than the 4-fluoro derivative (8). Chloro-substitution resulted in a compound (9) with better activity than the fluoro derivatives. Bromo derivatives (10 and 11) are both potent antimicrobial agents, and the 4-chloro (9) showed similar antimicrobial activity. The carboxylic acid functional group eliminated the activity of the resultant compounds (12 and 13).

Table 1. Synthesis of 3,5-bis(trifluoromethylphenyl)-derived pyrazole anilines.

#	R	HRMS (M + H) ⁺	Yield (%)	#	R	HRMS (M + H) ⁺	Yield (%)
1		506.1291	86	16		598.0553	82
2		548.1761	80	17		542.1122	83
3		562.1919	93	18		558.0816	90
4		536.1397	77	19		560.0776	86
5		598.1556	79	20		574.0509	85
6		552.1173	70	21		619.9990	92
7		524.1208	82	22		592.1082	86

Table 1. Cont.

8		524.1200	84	23		652.0280	83
9		540.0907	72	24		560.1030	77
10		584.0410	85	25		560.1026	76
11		584.0408	78	26		576.0721	83
12		550.1194	83	27		576.0729	69
13		550.1197	82	28		592.0402	90
14		538.1356	92	29		637.9897	88
15		554.1065	81	30		610.0322	67

We found the disubstituted aniline derivatives as potent antibacterial compounds. Both methyl and halogen-substituted compounds (**14**, **15**, and **16**) showed MIC values as low as 1 µg/mL. 4-Bromo-3-methyl derivative (**16**) appeared the most potent compound among these three derivatives. Tested bacteria were less susceptible to the difluorophenyl-substituted compound (**17**) with MIC values 1–4 µg/mL across the tested strains. Chloro-fluoro substitution (**18**) showed better activity than the difluoro derivative (**17**). Dichloro aniline derivatives (**19** and **20**) were among the most potent compounds in the series, with MIC values as low as 0.5 µg/mL. 4-Bromo-3-chloro-aniline-substituted pyrazole derivative (**21**) was very effective with MIC values as low as 0.5 µg/mL against *S. aureus*, including MRSA strains. Tested enterococci strains were also inhibited efficiently by this compound (**21**) with the MIC values of 1 µg/mL. Trifluoromethyl derivatives (**22** and **23**) showed good activity across the tested strains. Trifluoro aniline derivatives (**24** and **25**) were comparatively less potent than other trisubstituted derivatives. All the mixed trihalo derivatives (**26**, **27**, **28**, and **29**) showed good potency. Compound **26** inhibited the growth of many strains with MIC values as low as 0.25 µg/mL. The last compound (**30**) in the series was a good inhibitor of tested bacterial strains. The potency of most of the compounds was shown to be better than that of vancomycin and daptomycin, two widely used antibiotics to treat Gram-positive bacterial infections. Several compounds (e.g., **19**, **20**,

21, 22, 26, etc.) were up to 4 times more effective than these two positive controls against *S. aureus* strains. Some compounds (e.g., **3** and **19**) were more potent than vancomycin and daptomycin against *S. epidermidis* bacterium. Most of the compounds were very potent against the enterococci strains compared to the positive controls.

Table 2. MIC ($\mu\text{g}/\text{mL}$) data of the synthesized compounds. Gram-positive: Antibiotic susceptible *S. aureus* ATCC 25923 (Sa23), antibiotic-resistant (methicillin-resistant) strains: *S. aureus* BAA-2312 (Sa12), *S. aureus* ATCC 33591 (Sa91), *S. aureus* ATCC 33592 (Sa92), and *S. aureus* ATCC 700699 (Sa99); *S. epidermidis* ATCC 700296 (Se), antibiotic susceptible *E. faecalis* ATCC 29212 (Ef12), antibiotic-resistant (vancomycin-resistant, VRE) *E. faecalis* ATCC 51299 (Ef99), antibiotic-resistant (vancomycin-resistant, VRE) *E. faecium* ATCC 700221 (Ef21), *Bacillus subtilis* ATCC 6623 (Bs), V = Vancomycin and D = Daptomycin, $n = 3$.

#	Sa23	Sa12	Sa91	Sa92	Sa99	Se	Ef12	Ef99	Ef21	Bs
1	4	2	4	4	4	8	8	4	4	2
2	2	1	1	1	2	2	2	1	1	1
3	1	1	1	2	2	1	1	0.5	2	2
4	8	4	8	8	8	16	16	16	8	4
5	1	2	1	1	2	4	2	1	1	2
6	2	2	2	2	4	4	4	2	2	1
7	4	2	4	2	4	4	8	4	4	2
8	2	2	2	2	4	4	4	4	4	1
9	2	1	2	1	2	2	2	2	2	1
10	2	2	2	2	2	4	4	2	4	2
11	2	1	1	1	2	2	2	1	1	1
12	>32	>32	>32	>32	>32	>32	>32	>32	>32	>32
13	>32	32	>32	>32	>32	>32	>32	>32	>32	>32
14	2	1	2	1	2	4	2	2	1	1
15	2	1	1	2	2	2	2	2	1	1
16	1	1	1	1	2	2	1	2	1	1
17	2	2	2	2	2	4	4	4	2	1
18	2	1	1	1	2	2	2	2	1	1
19	1	0.5	0.5	1	2	1	1	1	1	1
20	1	1	0.5	1	1	2	1	1	1	1
21	1	1	0.5	0.5	2	2	1	1	1	1
22	1	1	1	1	1	2	2	2	1	2
23	1	2	1	1	2	4	2	2	2	1
24	2	1	1	1	2	4	2	2	1	1
25	4	2	2	2	4	4	4	4	2	1
26	2	0.25	2	1	1	4	1	2	0.25	0.25
27	1	1	1	1	2	2	2	2	1	1
28	1	1	1	1	1	2	2	2	1	1
29	2	1	1	1	2	2	2	2	1	2
30	1	2	1	1	2	2	2	2	1	1
V	1	0.5	2	2	4	2	2	>32	>32	0.25
D	2	2	2	2	8	2	16	16	16	2

Based on the activities, we found a good Structure Activity Relationship (SAR) of the product with respect to the substituents in the aniline moiety. The presence of a protic substituent, carboxylic acid, eliminated the activity of the compounds (**12** and **13**), which is in accordance with our previous findings [29,31,32]. The presence of lipophilic substituents ($\text{clog } P = 7\text{--}8$) on the phenyl ring of the aniline moiety increased the activity. As can be seen from the activity of mono-substituted compounds (**2**–**11**), the methoxy substituent is the least lipophilic ($\text{clog } P = 6.63$), and the corresponding compound (**4**) is the least potent for its antibacterial activity. *Para* isomers (**8** and **11**) are more potent than the corresponding *meta* products (**7** and **10**). Similar SAR was observed for disubstituted derivatives (**14**–**23**). Trisubstituted (**24**–**29**) and tetrasubstituted (**30**) compounds showed similar average activity as the disubstituted compounds.

2.1. Cytotoxicity Studies

After determining a high level of potency for several compounds, we tested them for their possible toxicity to cultured human cells (HEK-293) to select the least toxic compounds for further studies. Initially, compounds were tested at 50 and 25 $\mu\text{g}/\text{mL}$. Unfortunately, several compounds showed a toxic effect on HEK-293 cells. Compounds allowing >20% viability of HEK-293 cells at the tested concentrations were selected to test their toxicity at lower concentrations by determining their IC_{50} values (Figure 2). Compound 5 was the least toxic with an IC_{50} value of 9.15 $\mu\text{g}/\text{mL}$. Compounds 11, 28, and 29 inhibited the growth of these cells with IC_{50} values in the range of 7–8 $\mu\text{g}/\text{mL}$.

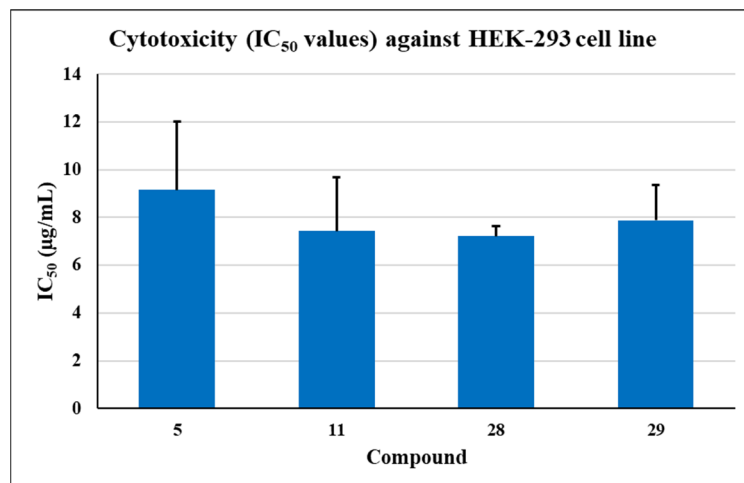


Figure 2. Cytotoxicity of potent antimicrobials for human embryonic kidney (HEK-293) cells. The data show the average of the IC_{50} values obtained from triplicate assays for each compound. Error bars indicate the standard deviation values ($n = 3$).

2.2. Time Kill Assay

Time Kill Assay studies give an idea of whether antibacterial agents are bactericidal or bacteriostatic. As can be seen in Figure 3, all four compounds were bactericidal, reducing bacterial concentrations 99.9% by 4 h and eliminating viable cells by 6 to 8 h. The positive controls, vancomycin (V) and daptomycin (D), eliminated >99.9% CFUs in 8 and 6 h, respectively. The negative control, DMSO, showed exponential growth as expected.

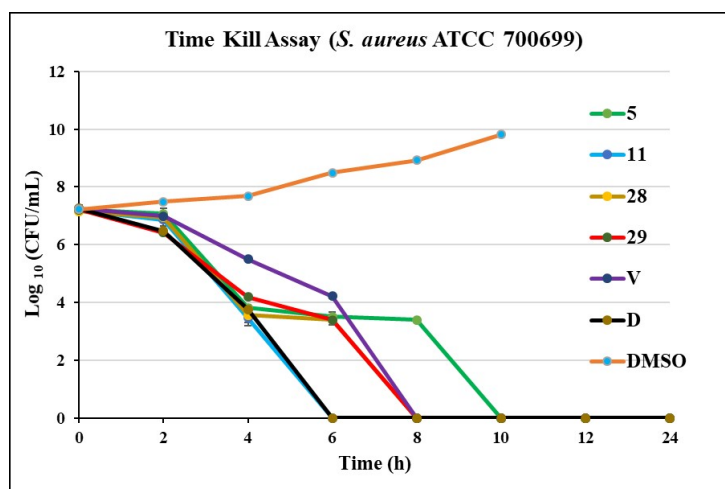


Figure 3. Time Kill Assay of potent compounds 5, 11, 28, and 29 against an MRSA (*S. aureus* ATCC 700699), Vancomycin (V), and Daptomycin (D) are positive controls. All compounds, including positive controls, were tested at a $4\times$ MIC concentration.

2.3. Activity against Persisters

Persisters are a nongrowing, antibiotic-tolerant state of bacteria. MRSA persisters are one of the major contributors to its virulence and lethality. Recently, a number of efforts are being made to eliminate MRSA persisters by using novel antibiotics [33–35]. In our effort to get potent anti-MRSA agents, we tested our promising compounds for their potency against persisters. Three of the four potent compounds (5, 11, 28, and 29) are very effective against *S. aureus* ATCC 700699 persisters. Compound 5 showed partial activity against the persisters (Figure 4). Compounds 11 and 29 were very effective at eliminating the persisters at $32\times$ MIC value. Compared to the positive controls, these two compounds reduced the population of persisters by 4 log values. Compound 28 is also very effective against the persisters, but less potent than of compounds 11 and 29. Conventional antibiotics, vancomycin and daptomycin, failed to demonstrate persister kill activity at $32\times$ MIC. Compounds 11 and 29 were further studied to examine the time-kill pattern during an 8 h period at various MIC concentrations (Figure 4b,c). Both compounds 11 and 29 eradicated more than 3 log values within an 8 h time course at all the $4\times$ MIC, $8\times$ MIC, and $16\times$ MIC concentrations, demonstrating excellent bactericidal activity against MRSA persisters. The $2\times$ MIC concentration of compound 11 eliminated 1 log value of the cells, while $2\times$ MIC of compound 29 demonstrated almost 2 log values decrease of persister cells in 8 h time period. The level of detection in this experiment was 2×10^4 CFU/mL, and the data point on $\log_{10} 4$ in the graph was below the level of detection (Figure 4a–c).

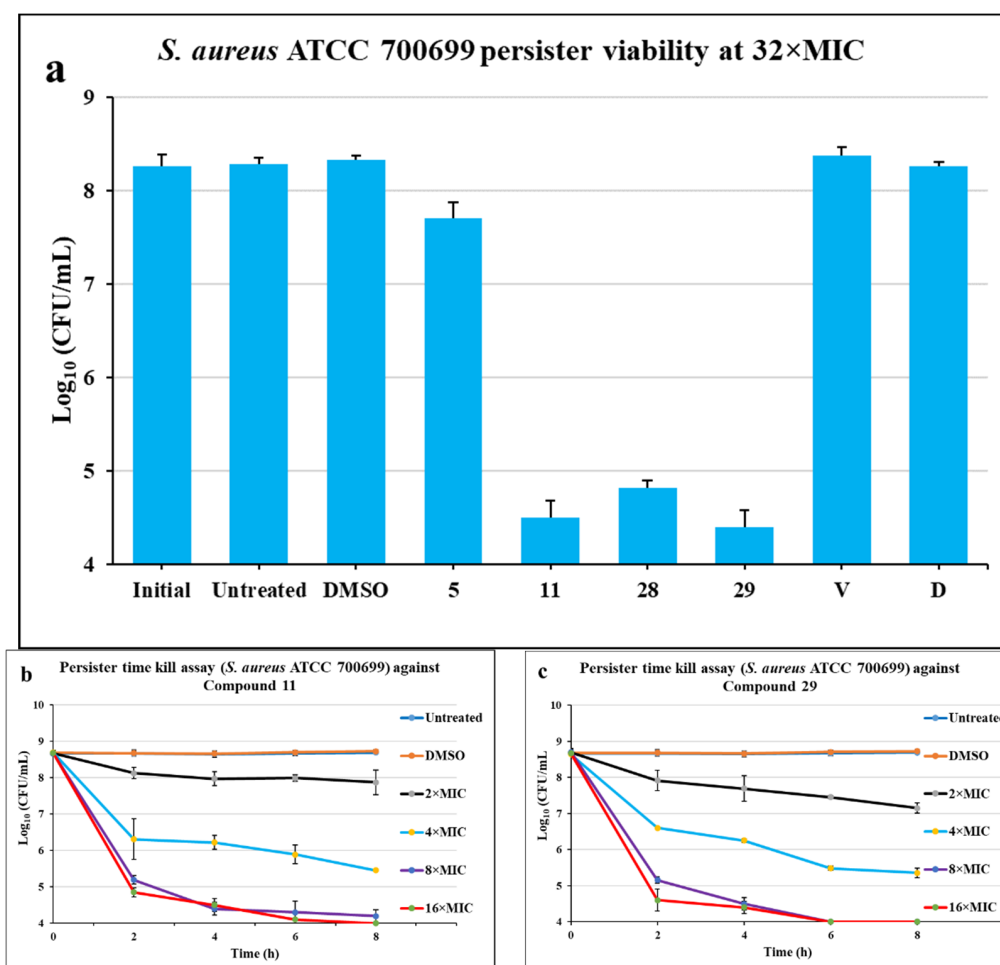


Figure 4. The activity of potent compounds against MRSA persisters. (a) Persister viability assay at $32\times$ MIC for each compound run for 4 h. Persister Time Kill Assay against (b) compound 11 and (c) compound 29 at various MIC values run for 8 h. The error bars represent the standard deviation of the colony count performed in triplicates for each treatment, $n = 3$.

2.4. Activity against *S. aureus* and *E. faecalis* Biofilms

Microbial biofilms are self-synthesized polymeric matrices that help microbial populations adhere to abiotic and biotic surfaces. Biofilms make bacteria recalcitrant to antibiotic treatment and protection from the host immune system. Biofilms formed by staphylococci (mostly by *S. epidermidis* and *S. aureus*) are the most common cause of device-related infections in hospital settings [7]. Enterococci biofilms are also frequently observed in the dysbiotic gastrointestinal tract, endocarditis, and wounds [4].

We tested the compounds showing potent activity against planktonic bacterial strains for their ability to eradicate the *S. aureus* and *E. faecalis* biofilms by using the Calgary Biofilm Device. As shown in Table 3, compound **11** showed potent antibiofilm property with the MBEC values 2 and 4 µg/mL against *S. aureus* and *E. faecalis*, respectively. Compounds **28** and **29** are even better with MBEC values that are as low as 1 µg/mL. Compound **5** did not show any appreciable biofilm eradication property. Comparing with the positive control, vancomycin (**V**) and daptomycin (**D**), our compounds (**11**, **28**, and **29**) are very potent in eradicating the *S. aureus* and *E. faecalis* biofilms.

Table 3. Biofilm studies of potent compounds.

#	MBEC (µg/mL)	
	Sa23	Efs12
5	>32	>32
11	2	4
28	1	2
29	2	2
V	>32	>32
D	>32	>32

3. Procedures

3.1. General Consideration

All of the reactions were carried out under an air atmosphere in round-bottom flasks. All reactant materials, solvents, deuterated solvents for ^1H and ^{13}C Nuclear Magnetic Resonance (NMR) spectroscopy, and for the reactions were purchased from Fisher Scientific (Hanover Park, IL, USA) and Oakwood chemical (Estill, SC, USA). ^1H and ^{13}C NMR spectra were recorded on a Varian Mercury with 300 MHz for ^1H and 75 MHz for ^{13}C NMR. The Fourier Transform Infrared (FTIR) spectra were obtained using 7 mm KBr pellets for the specimen using a Nicolet™ iS™ 10 FTIR spectrometer (Thermo Fisher Scientific Inc., Waltham, MA, USA). High Resolution Mass Spectrometry (HRMS) data were obtained by using the Bruker Apex II-FTMS system.

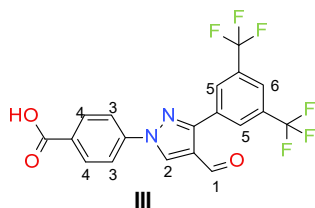
3.2. Synthesis of 3,5-Bis(trifluoromethyl)phenyl-derived Pyrazole Aldehyde (**III**)

4-Hydrazinobenzoic acid (1.597 g, 10.5 mmol) and 3,5-bis(trifluoromethyl)acetophenone (2.561 g, 10 mmol) were taken in a 100 mL round-bottom flask. Anhydrous ethanol (50 mL) was added to the flask, and the reaction mixture was refluxed for 8 h. After completing the reaction, the solvent was removed under reduced pressure using a rotary evaporator, resulting in a dry product. Then 30 mL anhydrous *N,N*-dimethylformamide (DMF) was added to the flask and sealed with a septum followed by stirring for 15 min to dissolve the compound. After getting a clear solution, the flask was cooled using an ice bath. Then phosphorous oxychloride, POCl_3 (4.67 mL, 50 mmol) was added dropwise using a syringe through the septum. After 30 min, the mixture was brought to ambient temperature and heated at 90 °C for 8 h. Then, the reaction mixture was poured into an ice-full beaker (300 mL) and stirred for 10 h to make precipitate. The precipitate was filtered and washed with water several times. Drying under vacuum gave the final pure 3,5-bis(trifluoromethyl)phenyl-derived pyrazole aldehyde (**III**).

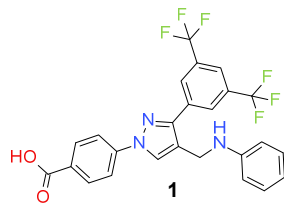
3.3. Synthesis of 3,5-Bis(trifluoromethyl)phenyl Substituted Pyrazole-Derived Anilines (1–30)

The pyrazole aldehyde (214.14 mg, 0.5 mmol) and 0.55 mmol aniline derivative were taken in a round-bottom flask and refluxed in toluene for 6 h in a Dean-Stark condenser. Then, the reaction mixture was cooled and filtered under vacuum. The precipitate was recrystallized in acetonitrile to give a pure imine product. The imine product (0.5 mmol) was dissolved in methanol and cooled to 0 °C using an ice bath. NaBH₄ (94.5 mg, 2.5 mmol) was added to the solution before stirring the mixture for 10 h. After that 10% HCl was added to form the precipitate. The precipitate was recrystallized in acetonitrile to obtain the pure 3,5-bis(trifluoromethyl)phenyl substituted pyrazole-derived aniline product.

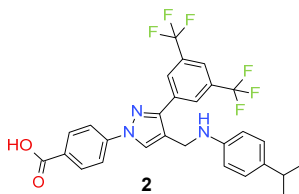
3.4. Compound Characterization Data



4-[3-[3,5-Bis(trifluoromethyl)phenyl]-4-formyl-pyrazol-1-yl] benzoic acid (**III**). Beige solid; (420 mg, 98%); IR (KBr pellet, cm⁻¹): 3095 (aromatic C-H), 2672, 1694 (C=O), 1608, 1131 (C-F); ¹H NMR, 300 MHz (DMSO-*d*₆): δ 9.96 (s, 1H, H-1), 9.58 (s, 1H, H-2), 8.70 (s, 2H, H-4), 8.21–8.11 (m, 5H, H-3, H-5 and H-6); ¹³C NMR (75 MHz, DMSO-*d*₆): δ 184.8, 166.9, 162.7, 149.3, 141.6, 138.7, 133.9 (³J_{C-F} = 4.0 Hz), 131.4, 130.8 (²J_{C-F} = 33.2 Hz), 129.4, 129.1, 123.7 (¹J_{C-F} = 270.6 Hz), 123.2, 119.5 (m). HRMS (ESI-FTMS Mass (*m/z*): calcd for C₁₉H₁₀F₆N₂O₃ [M + H]⁺ = 429.0668, found 429.0747. (Supplementary Materials)

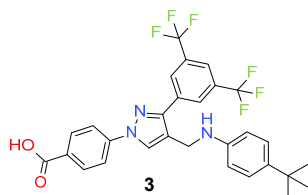


4-[4-(Anilinomethyl)-3-[3,5-bis(trifluoromethyl)phenyl]pyrazol-1-yl] benzoic acid (**1**). Light beige solid; (436 mg, 86%); IR (KBr pellet, cm⁻¹): 3415, 2894, 1699, 1608, 1360, 1316, 1278, 1174, 1134; ¹H NMR, 300 MHz (DMSO-*d*₆): δ 8.92 (s, 1H), 8.22 (s, 2H), 8.09–7.98 (m, 5H), 7.15 (d, *J* = 7.4 Hz, 2H), 7.00–6.92 (m, 3H), 4.45 (s, 2H); ¹³C NMR (75 MHz, DMSO-*d*₆): δ 167.0, 149.8, 142.3, 135.0, 132.0, 131.5, 130.8 (²J_{C-F} = 32.9 Hz), 130.3, 129.6, 129.3, 129.0, 128.5, 123.6 (¹J_{C-F} = 270.2 Hz), 122.1, 118.6, 116.4, 41.9. HRMS (ESI-FTMS Mass (*m/z*): calcd for C₂₅H₁₇F₆N₃O₂ [M + H]⁺ = 506.1298, found 506.1291.

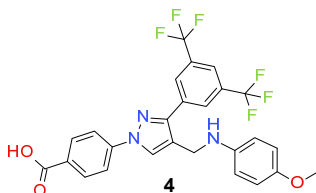


4-[3-[3,5-Bis(trifluoromethyl)phenyl]-4-[(4-isopropylanilino)methyl]pyrazol-1-yl] benzoic acid (**2**). Light beige solid; (443 mg, 80%); IR (KBr pellet, cm⁻¹): 3411, 2969, 1714, 1607, 1358, 1281, 1172, 1127; ¹H NMR, 300 MHz (DMSO-*d*₆): δ 8.92 (s, 1H), 8.31 (s, 2H), 8.06 (t, *J* = 8.7 Hz, 5H), 7.08 (d, *J* = 8.0 Hz, 2H), 6.94 (br, 2H), 4.48 (s, 2H), 2.75–2.73 (m, 1H), 1.11 (d, *J* = 6.7 Hz, 6H); ¹³C NMR (75 MHz, DMSO-*d*₆): δ 167.0, 149.5, 142.3, 135.1, 132.1, 131.6, 131.0 (²J_{C-F} = 32.8 Hz), 130.4, 129.3, 129.0, 128.4, 127.4, 123.6 (¹J_{C-F} = 271.2 Hz), 122.1, 118.6, 118.2,

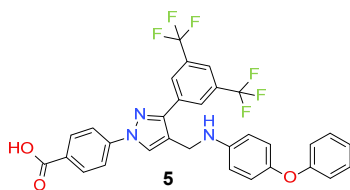
43.0, 33.1, 24.1. HRMS (ESI-FTMS Mass (m/z): calcd for $C_{28}H_{23}F_6N_3O_2$ [$M + H$] $^+$ = 548.1767, found 548.1761.



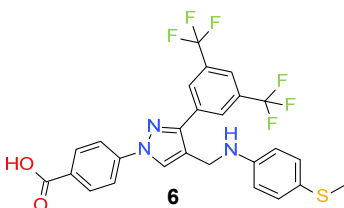
4-[3-[3,5-Bis(trifluoromethyl)phenyl]-4-[(4-tert-butylanilino)methyl]pyrazol-1-yl] benzoic acid (**3**). White solid; (526 mg, 93%); IR (KBr pellet, cm^{-1}): 3419, 2969, 1712, 1607, 1357, 1281, 1178, 1131; 1H NMR, 300 MHz (DMSO- d_6): δ 8.92 (s, 1H), 8.32 (s, 2H), 8.06 (t, $J = 8.4$ Hz, 5H), 7.23 (d, $J = 8.0$ Hz, 2H), 6.95 (d, $J = 7.3$ Hz, 2H), 4.49 (s, 2H), 1.18 (s, 9H); ^{13}C NMR (75 MHz, DMSO- d_6): δ 167.0, 149.5, 142.3, 135.1, 132.2, 131.6, 131.2, 130.8 ($^2J_{C-F} = 32.6$ Hz), 130.4, 129.4, 128.3, 126.4, 123.6 ($^1J_{C-F} = 271.2$ Hz), 122.2, 118.6, 118.2, 43.0, 34.4, 31.4. HRMS (ESI-FTMS Mass (m/z): calcd for $C_{29}H_{25}F_6N_3O_2$ [$M + H$] $^+$ = 562.1924, found 562.1919.



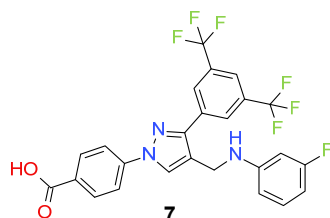
4-[3-[3,5-Bis(trifluoromethyl)phenyl]-4-[(4-methoxyanilino)methyl]pyrazol-1-yl] benzoic acid (**4**). Light grey solid; (417 mg, 77%); IR (KBr pellet, cm^{-1}): 3219, 2261, 1701, 1608, 1280, 1074, 1032; 1H NMR, 300 MHz (DMSO- d_6): δ 9.03 (s, 1H), 8.09 (t, $J = 9.3$ Hz, 5H), 7.99 (d, $J = 8.4$ Hz, 2H), 7.11 (d, $J = 8.4$ Hz, 2H), 6.72 (d, $J = 8.5$ Hz, 2H), 4.59 (s, 2H), 3.63 (s, 3H); ^{13}C NMR (75 MHz, DMSO- d_6): δ 166.9, 150.4, 142.2, 134.8, 133.1, 131.6, 130.6 ($^2J_{C-F} = 32.7$ Hz), 129.5, 129.0, 128.7, 124.9, 123.6 ($^1J_{C-F} = 271.2$ Hz), 118.7, 118.1, 115.2, 114.7, 55.5, 44.6. HRMS (ESI-FTMS Mass (m/z): calcd for $C_{26}H_{19}F_6N_3O_3$ [$M + H$] $^+$ = 536.1403, found 536.1397.



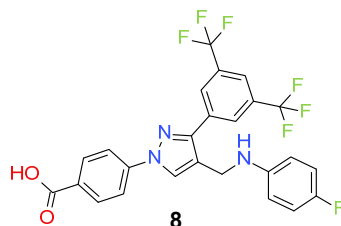
4-[3-[3,5-Bis(trifluoromethyl)phenyl]-4-[(4-phenoxyanilino)methyl]pyrazol-1-yl] benzoic acid (**5**). Off white solid; (477 mg, 79%); IR (KBr pellet, cm^{-1}): 3416, 2749, 1692, 1607, 1313, 1179, 1140; 1H NMR, 300 MHz (DMSO- d_6): δ 8.95 (s, 1H), 8.32 (s, 2H), 8.14–8.03 (m, 5H), 7.34 (t, $J = 7.4$ Hz, 2H), 7.11–7.01 (m, 3H), 6.88 (t, $J = 7.6$ Hz, 4H), 4.47 (s, 2H); ^{13}C NMR (75 MHz, DMSO- d_6): δ 167.0, 157.7, 149.6, 142.3, 135.1, 132.0, 131.5, 131.1 ($^2J_{C-F} = 32.7$ Hz), 130.3, 129.3, 128.6, 128.4, 125.5, 123.6 ($^1J_{C-F} = 271.2$ Hz), 123.4, 122.1, 120.3, 119.8, 119.4, 118.6, 118.1. HRMS (ESI-FTMS Mass (m/z): calcd for $C_{31}H_{21}F_6N_3O_3$ [$M + H$] $^+$ = 598.1560, found 598.1556.



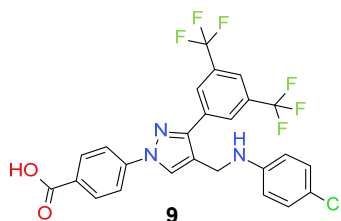
4-[3-[3,5-Bis(trifluoromethyl)phenyl]-4-(4-methylsulfanylanilino)methyl]pyrazol-1-yl] benzoic acid (**6**). Light yellow solid; (389 mg, 70%); IR (KBr pellet, cm^{-1}): 3412, 2924, 1701, 1608, 1359, 1281, 1177, 1131; ^1H NMR, 300 MHz (DMSO- d_6): δ 8.93 (s, 1H), 8.29 (s, 2H), 8.12–8.02 (m, 5H), 7.10 (d, $J = 8.5$ Hz, 2H), 6.91 (d, $J = 8.3$ Hz, 2H), 4.44 (s, 2H), 2.36 (s, 3H); ^{13}C NMR (75 MHz, DMSO- d_6): δ 167.0, 149.3, 142.4, 135.2, 131.5, 130.9 ($^2J_{\text{C-F}} = 32.8$ Hz), 129.4, 129.2, 129.0, 128.2, 127.2, 124.2, 123.6 ($^1J_{\text{C-F}} = 271.3$ Hz), 122.1, 119.5, 118.5, 118.2, 17.2. HRMS (ESI-FTMS Mass (m/z): calcd for $\text{C}_{26}\text{H}_{19}\text{F}_6\text{N}_3\text{O}_2\text{S}$ [$\text{M} + \text{H}$] $^+$ = 552.1175, found 552.1173.



4-[3-[3,5-Bis(trifluoromethyl)phenyl]-4-(3-fluoroanilino)methyl]pyrazol-1-yl] benzoic acid (**7**). White solid; (433 mg, 82%); IR (KBr pellet, cm^{-1}): 3420, 2903, 1699, 1608, 1359, 1281, 1175, 1134; ^1H NMR, 300 MHz (DMSO- d_6): δ 8.84 (s, 1H), 8.40 (s, 2H), 8.07–8.11 (m, 5H), 7.10 (d, $J = 7.05$ Hz, 1H), 6.50 (t, $J = 7.4$ Hz, 2H), 6.38–6.29 (m, 1H), 4.29 (s, 2H); ^{13}C NMR (75 MHz, DMSO- d_6): δ 167.0, 163.7 (d, $^1J_{\text{C-F}} = 238.4$ Hz), 150.2 (d, $^3J_{\text{C-F}} = 10.9$ Hz), 148.9, 142.4, 135.3, 131.4 ($^3J_{\text{C-F}} = 4.6$ Hz), 131.0, 130.7 (d, $^3J_{\text{C-F}} = 10.2$ Hz), 129.1, 127.9, 123.6 ($^1J_{\text{C-F}} = 271.2$ Hz), 122.0, 119.9, 118.4, 109.5, 103.4 (d, $^2J_{\text{C-F}} = 20.8$ Hz), 99.4 (d, $^2J_{\text{C-F}} = 24.8$ Hz), 38.3. HRMS (ESI-FTMS Mass (m/z): calcd for $\text{C}_{25}\text{H}_{16}\text{F}_7\text{N}_3\text{O}_2$ [$\text{M} + \text{H}$] $^+$ = 524.1204, found 524.1208.

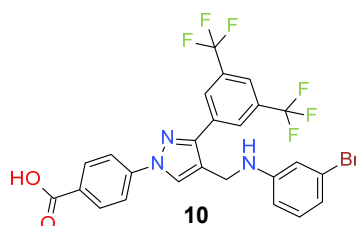


4-[3-[3,5-Bis(trifluoromethyl)phenyl]-4-(4-fluoroanilino)methyl]pyrazol-1-yl] benzoic acid (**8**). Off white solid; (443 mg, 84%); IR (KBr pellet, cm^{-1}): 3413, 2970, 1712, 1607, 1357, 1281, 1178, 1131; ^1H NMR, 300 MHz (DMSO- d_6): δ 8.92 (s, 1H), 8.26 (s, 2H), 8.09–8.04 (m, 5H), 6.99 (d, $J = 6.7$ Hz, 4H), 4.44 (s, 2H); ^{13}C NMR (75 MHz, DMSO- d_6): δ 167.0, 158.3 (d, $^1J_{\text{C-F}} = 236.5$ Hz), 149.7, 142.3, 138.8, 135.0, 132.0, 131.7, 131.0 ($^2J_{\text{C-F}} = 32.8$ Hz), 129.3, 128.4, 125.4, 121.9 (d, $^2J_{\text{C-F}} = 21.5$ Hz), 121.4 ($^1J_{\text{C-F}} = 280.7$ Hz), 118.6, 116.2 (d, $^2J_{\text{C-F}} = 22.4$ Hz), 41.6. HRMS (ESI-FTMS Mass (m/z): calcd for $\text{C}_{25}\text{H}_{16}\text{F}_7\text{N}_3\text{O}_2$ [$\text{M} + \text{H}$] $^+$ = 524.1204, found 524.1200.

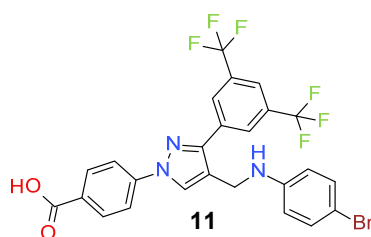


4-[3-[3,5-Bis(trifluoromethyl)phenyl]-4-(4-chloroanilino)methyl]pyrazol-1-yl] benzoic acid (**9**). Yellowish white solid; (391 mg, 72%); IR (KBr pellet, cm^{-1}): 3409, 2899, 1699, 1608, 1359, 1286, 1178, 1130; ^1H NMR, 300 MHz (DMSO- d_6): δ 8.84 (s, 1H), 8.39 (s, 2H), 8.12–8.07 (m, 5H), 7.13 (d, $J = 8.4$ Hz, 2H), 6.73 (d, $J = 8.6$ Hz, 2H), 4.29 (s, 2H); ^{13}C NMR (75 MHz, DMSO- d_6): δ 167.0, 149.0, 146.5, 142.4, 135.3, 131.4 ($^3J_{\text{C-F}} = 7.1$ Hz), 130.8 ($^2J_{\text{C-F}} = 42.8$ Hz), 129.1 (m), 128.0, 123.6 ($^1J_{\text{C-F}} = 271.1$ Hz), 123.2, 122.0, 121.3, 119.7, 118.5, 118.2, 115.1, 38.7.

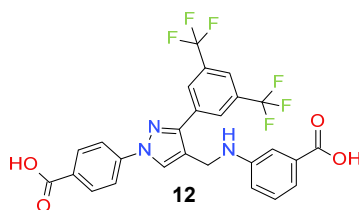
HRMS (ESI-FTMS Mass (m/z): calcd for $C_{25}H_{16}ClF_6N_3O_2$ [$M + H$] $^+$ = 540.0908, 542.0881, found 540.0907.



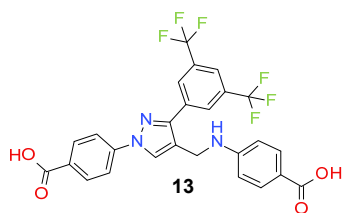
4-[3-[3,5-Bis(trifluoromethyl)phenyl]-4-[(3-bromoanilino)methyl]pyrazol-1-yl] benzoic acid (**10**). Off white solid; (497 mg, 85%); IR (KBr pellet, cm^{-1}): 3410, 3126, 1706, 1607, 1373, 1277, 1188, 1137; 1H NMR, 300 MHz (DMSO- d_6): δ 8.85 (s, 1H), 8.40 (s, 2H), 8.13–8.08 (m, 5H), 7.03 (t, $J = 7.8$ Hz, 1H), 6.86 (s, 1H), 6.73 (dd, $J = 7.8, 14.5$ Hz, 2H), 4.29 (s, 2H); ^{13}C NMR (75 MHz, DMSO- d_6): δ 167.0, 149.8, 148.9, 142.4, 135.3, 131.8, 131.5, 130.9, 130.5, 129.1, 127.9, 123.6 ($^1J_{C-F} = 271.1$ Hz), 122.7, 122.0, 119.7 ($^2J_{C-F} = 26.2$ Hz), 118.4, 115.2, 112.1, 38.1. HRMS (ESI-FTMS Mass (m/z): calcd for $C_{25}H_{16}BrF_6N_3O_2$ [$M + H$] $^+$ = 584.0403, 586.0384, found 584.0410.



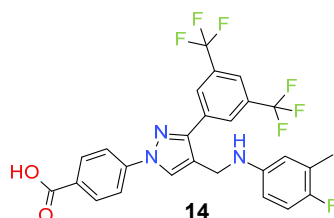
4-[3-[3,5-Bis(trifluoromethyl)phenyl]-4-[(4-bromoanilino)methyl]pyrazol-1-yl] benzoic acid (**11**). Yellow solid; (457 mg, 78%); IR (KBr pellet, cm^{-1}): 3377, 3072, 1712, 1607, 1356, 1282, 1178, 1128; 1H NMR, 300 MHz (DMSO- d_6): δ 8.83 (s, 1H), 8.40 (s, 2H), 8.12–8.04 (m, 5H), 7.24 (d, $J = 8.6$ Hz, 2H), 6.67 (d, $J = 8.7$ Hz, 2H), 4.27 (s, 2H); ^{13}C NMR (75 MHz, DMSO- d_6): δ 167.0, 149.0, 147.2, 142.4, 135.3, 131.6 ($^2J_{C-F} = 34.7$ Hz), 131.0 ($^3J_{C-F} = 4.0$ Hz), 130.5, 129.1, 127.9, 123.6 ($^1J_{C-F} = 271.2$ Hz), 123.2, 122.0, 119.8, 118.4, 115.4, 108.4, 38.5. HRMS (ESI-FTMS Mass (m/z): calcd for $C_{25}H_{16}BrF_6N_3O_2$ [$M + H$] $^+$ = 584.0403, 586.0384, found 584.0408.



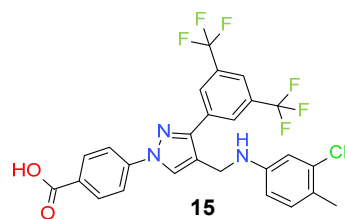
3-[3-[3,5-Bis(trifluoromethyl)phenyl]-1-(4-carboxyphenyl)pyrazol-4-yl]methylamino benzoic acid (**12**). Light gold solid; (458 mg, 83%); IR (KBr pellet, cm^{-1}): 3361, 3064, 1685, 1604, 1520, 1176, 1132; 1H NMR, 300 MHz (DMSO- d_6): δ 8.84 (s, 1H), 8.43 (s, 2H), 8.12–8.08 (m, 5H), 7.28–7.20 (m, 3H), 6.92 (s, 1H), 6.33 (br, 1H), 4.32 (s, 2H); ^{13}C NMR (75 MHz, DMSO- d_6): δ 168.3, 167.0, 148.9, 148.6, 142.4, 135.3, 131.8, 131.4 ($^3J_{C-F} = 4.5$ Hz), 130.8 ($^2J_{C-F} = 32.7$ Hz), 129.4, 129.0, 127.9, 123.6 ($^1J_{C-F} = 271.2$ Hz), 122.0, 120.3, 118.4, 118.2, 118.0, 116.9, 113.5, 38.2. HRMS (ESI-FTMS Mass (m/z): calcd for $C_{26}H_{17}F_6N_3O_4$ [$M + H$] $^+$ = 550.1196, found 550.1194.



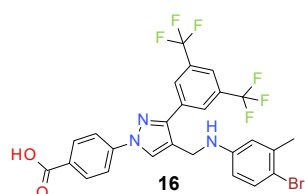
4-[[3-[3,5-Bis(trifluoromethyl)phenyl]-1-(4-carboxyphenyl)pyrazol-4-yl]methylamino] benzoic acid (**13**). Light yellow solid; (451 mg, 82%); IR (KBr pellet, cm^{-1}): 3361, 2667, 1686, 1601, 1419, 1282, 1178; ^1H NMR, 300 MHz (DMSO- d_6): δ 8.84 (s, 1H), 8.39 (s, 2H), 8.13–8.08 (m, 5H), 7.71 (d, $J = 7.1$ Hz, 2H), 6.83 (s, 1H), 6.70 (d, $J = 8.6$ Hz, 2H), 4.36 (s, 2H); ^{13}C NMR (75 MHz, DMSO- d_6): δ 167.9, 167.0, 152.3, 148.9, 142.4, 135.3, 132.8, 131.5 ($^3J_{\text{C-F}} = 4.2$ Hz), 130.8 ($^2J_{\text{C-F}} = 32.5$ Hz), 129.1, 129.0, 127.9, 123.6 ($^1J_{\text{C-F}} = 271.2$ Hz), 122.1, 119.9, 118.5, 118.2, 111.7, 37.7. HRMS (ESI-FTMS Mass (m/z): calcd for $\text{C}_{26}\text{H}_{17}\text{F}_6\text{N}_3\text{O}_4$ [$\text{M} + \text{H}$] $^+$ = 550.1196, found 550.1197.



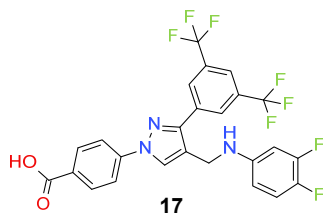
4-[[3-[3,5-Bis(trifluoromethyl)phenyl]-1-(4-fluoro-3-methyl-anilino)methyl]pyrazol-1-yl] benzoic acid (**14**). White solid; (497 mg, 92%); IR (KBr pellet, cm^{-1}): 3424, 2906, 1698, 1608, 1358, 1281, 1177, 1139; ^1H NMR, 300 MHz (DMSO- d_6): δ 8.94 (s, 1H), 8.21 (s, 2H), 8.05 (t, $J = 8.6$ Hz, 5H), 6.94–6.83 (m, 3H), 4.48 (s, 2H), 2.04 (s, 3H); ^{13}C NMR (75 MHz, DMSO- d_6): δ 167.0, 158.3 ($^1J_{\text{C-F}} = 240.57$ Hz), 150.0, 142.3, 134.9, 132.4, 131.5, 130.7 ($^2J_{\text{C-F}} = 32.7$ Hz), 130.3, 129.4, 128.5, 125.6, 123.6 ($^1J_{\text{C-F}} = 271.11$ Hz), 122.1, 118.6, 118.1, 115.9 (d, $^2J_{\text{C-F}} = 23.5$ Hz), 39.0, 14.5. HRMS (ESI-FTMS Mass (m/z): calcd for $\text{C}_{26}\text{H}_{18}\text{F}_7\text{N}_3\text{O}_2$ [$\text{M} + \text{H}$] $^+$ = 538.1360, found 538.1356.



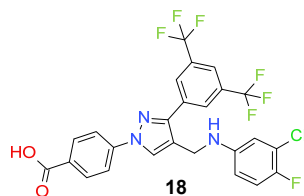
4-[[3-[3,5-Bis(trifluoromethyl)phenyl]-1-(3-chloro-4-methyl-anilino)methyl]pyrazol-1-yl] benzoic acid (**15**). Light brown solid; (453 mg, 81%); IR (KBr pellet, cm^{-1}): 3366, 2930, 1724, 1608, 1405, 1277, 1177, 1128; ^1H NMR, 300 MHz (DMSO- d_6): δ 8.93 (s, 1H), 8.26 (s, 2H), 8.08–7.99 (m, 5H), 7.07 (d, $J = 8.2$ Hz, 1H), 6.95 (s, 1H), 6.80 (d, $J = 8.0$ Hz, 1H), 4.39 (s, 2H), 2.12 (s, 3H); ^{13}C NMR (75 MHz, DMSO- d_6): δ 166.9, 149.4, 142.3, 135.0, 133.8, 132.0, 131.8, 131.5, 130.8 ($^2J_{\text{C-F}} = 32.7$ Hz), 129.2, 129.0, 128.2, 123.6 ($^1J_{\text{C-F}} = 271.1$ Hz), 121.9, 118.5, 118.1, 117.5, 117.0, 116.6, 19.0. HRMS (ESI-FTMS Mass (m/z): calcd for $\text{C}_{26}\text{H}_{18}\text{F}_6\text{N}_3\text{O}_2\text{Cl}$ [$\text{M} + \text{H}$] $^+$ = 554.1065, 556.1037, found 554.1065.



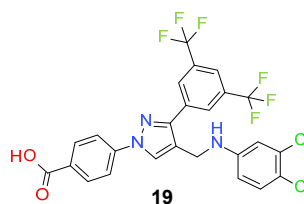
4-[3-[3,5-Bis(trifluoromethyl)phenyl]-4-[(4-bromo-3-methyl-anilino)methyl]pyrazol-1-yl] benzoic acid (**16**). Yellowish white solid; (489 mg, 82%); IR (KBr pellet, cm^{-1}): 2930, 1683, 1607, 1355, 1277, 1134; ^1H NMR, 300 MHz (DMSO- d_6): δ 8.84 (s, 1H), 8.25 (s, 2H), 8.03–7.99 (m, 5H), 7.24 (d, $J = 8.5$ Hz, 1H), 6.80 (s, 1H), 6.61 (d, $J = 7.9$ Hz, 1H), 4.33 (s, 2H), 2.12 (s, 3H); ^{13}C NMR (75 MHz, DMSO- d_6): δ 167.0, 149.3, 143.8, 142.3, 138.0, 135.1, 132.8, 131.7, 131.4, 130.8 ($^2J_{\text{C-F}} = 32.7$ Hz), 129.2, 129.0, 128.1, 123.5 ($^1J_{\text{C-F}} = 271.2$ Hz), 118.8, 118.4, 118.1, 117.7, 116.2, 22.9. HRMS (ESI-FTMS Mass (m/z): calcd for $\text{C}_{26}\text{H}_{18}\text{BrF}_6\text{N}_3\text{O}_2$ [$\text{M} + \text{H}$] $^+$ = 598.0559, 600.0540, found 598.0553.



4-[3-[3,5-Bis(trifluoromethyl)phenyl]-4-[(3,4-difluoroanilino)methyl]pyrazol-1-yl] benzoic acid (**17**). White solid; (449 mg, 83%); IR (KBr pellet, cm^{-1}): 3412, 2802, 1701, 1608, 1358, 1281, 1174, 1139; ^1H NMR, 300 MHz (DMSO- d_6): δ 8.83 (s, 1H), 8.35 (s, 2H), 8.08–8.05 (m, 5H), 7.19–7.09 (m, 1H), 6.74–6.71 (m, 1H), 6.51 (d, $J = 6.6$ Hz, 1H), 4.26 (s, 2H); ^{13}C NMR (75 MHz, DMSO- d_6): δ 167.0, 150.3 (dd, $J_{\text{C-F}} = 13.1, 233.8$ Hz), 149.0, 144.9 (d, $^3J_{\text{C-F}} = 8.5$ Hz), 142.5 (dd, $J_{\text{C-F}} = 13.0, 239.0$ Hz), 142.4, 135.2, 131.8, 131.4 ($^3J_{\text{C-F}} = 5.3$ Hz), 130.8 ($^2J_{\text{C-F}} = 32.6$ Hz), 129.1, 127.9, 123.6 ($^1J_{\text{C-F}} = 271.2$ Hz), 123.2, 121.9, 119.3, 118.4, 117.9 (d, $^2J_{\text{C-F}} = 17.4$ Hz), 109.7, 102.0 (d, $^2J_{\text{C-F}} = 20.2$ Hz). HRMS (ESI-FTMS Mass (m/z): calcd for $\text{C}_{25}\text{H}_{15}\text{F}_8\text{N}_3\text{O}_2$ [$\text{M} + \text{H}$] $^+$ = 542.1109, found 542.1122.

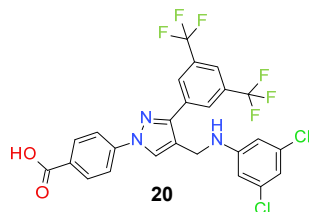


4-[3-[3,5-Bis(trifluoromethyl)phenyl]-4-[(3-chloro-4-fluoroanilino)methyl]pyrazol-1-yl] benzoic acid (**18**). Off white solid (506 mg, 90%); IR (KBr pellet, cm^{-1}): 3412, 2898, 1698, 1608, 1356, 1278, 1177, 1142. ^1H NMR, 300 MHz (DMSO- d_6): δ 8.85 (s, 1H), 8.34 (s, 2H), 8.09–8.05 (m, 5H), 7.14 (t, $J = 9.0$ Hz, 1H), 6.88 (s, 1H), 6.71 (d, $J = 8.8$ Hz, 1H), 4.29 (s, 2H); ^{13}C NMR (75 MHz, DMSO- d_6): δ 167.0, 150.8 (d, $^1J_{\text{C-F}} = 235.0$ Hz), 149.1, 144.3, 142.4, 135.2, 131.8, 131.4, 131.2 ($^2J_{\text{C-F}} = 32.7$ Hz), 130.5, 129.1 (d, $^3J_{\text{C-F}} = 10.5$ Hz), 128.0, 123.6 ($^1J_{\text{C-F}} = 271.2$ Hz), 122.0, 119.9 (d, $^2J_{\text{C-F}} = 18.1$ Hz), 119.0, 118.4, 117.4 (d, $^2J_{\text{C-F}} = 21.4$ Hz), 114.8. HRMS (ESI-FTMS Mass (m/z): calcd for $\text{C}_{25}\text{H}_{15}\text{ClF}_7\text{N}_3\text{O}_2$ [$\text{M} + \text{H}$] $^+$ = 558.0814, 560.0786, found 558.0816.

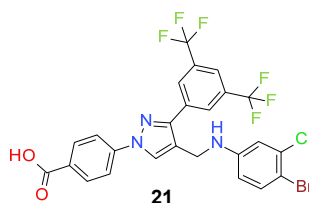


4-[3-[3,5-Bis(trifluoromethyl)phenyl]-4-[(3,4-dichloroanilino)methyl]pyrazol-1-yl] benzoic acid (**19**). Off white solid; (497 mg, 86%); IR (KBr pellet, cm^{-1}): 3403, 2866, 1682, 1607, 1359, 1278, 1143; ^1H NMR, 300 MHz (DMSO- d_6): δ 8.83 (s, 1H), 8.39 (s, 2H), 8.14–8.08 (m, 5H), 7.29 (d, $J = 8.7$ Hz, 1H), 6.88–6.87 (m, 1H), 6.66 (dd, $J = 2.5, 8.82$ Hz, 1H), 6.54–6.52 (m, 1H), 4.31–2.29 (m, 2H); ^{13}C NMR (75 MHz, DMSO- d_6): δ 167.0, 152.3, 148.8, 148.3, 146.1,

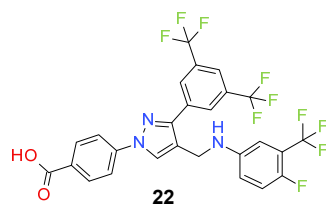
142.4, 135.2, 131.4, 130.7 ($^2J_{C-F} = 35.3$ Hz), 129.0, 127.8, 123.6 ($^1J_{C-F} = 266.3$ Hz), 120.0 ($^3J_{C-F} = 5.9$ Hz), 119.7, 118.3, 117.4, 117.1, 113.0, 112.6 (m), 38.4. HRMS (ESI-FTMS Mass (m/z): calcd for $C_{25}H_{15}Cl_2F_6N_3O_2$ [$M + H$] $^+$ = 574.0518, 576.0490, found 574.0776.



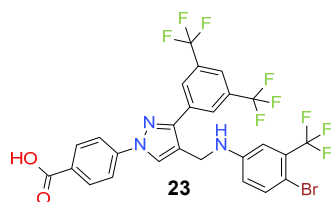
4-[3-[3,5-Bis(trifluoromethyl)phenyl]-4-[(3,5-dichloroanilino)methyl]pyrazol-1-yl] benzoic acid (**20**). Off white solid; (489 mg, 85%); IR (KBr pellet, cm^{-1}): 3425, 3090, 1697, 1607, 1362, 1281, 1186, 1138; 1H NMR, 300 MHz (DMSO- d_6): δ 8.82 (s, 1H), 8.36 (s, 2H), 8.12–8.07 (m, 5H), 6.67 (s, 4H), 4.32 (s, 2H); ^{13}C NMR (75 MHz, DMSO- d_6): δ 167.0, 150.7, 148.9, 142.4, 135.2, 134.8, 131.8, 131.4 ($^3J_{C-F} = 3.0$ Hz), 130.8 ($^2J_{C-F} = 32.8$ Hz), 129.1, 127.9, 123.6 ($^1J_{C-F} = 271.2$ Hz), 122.1, 119.8, 118.4, 115.4, 110.8, 37.8. HRMS (ESI-FTMS Mass (m/z): calcd for $C_{25}H_{15}Cl_2F_6N_3O_2$ [$M + H$] $^+$ = 574.0518, 576.0490, found 574.0509.



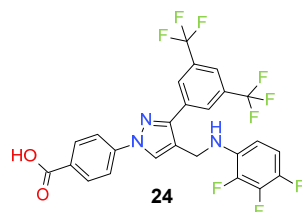
4-[3-[3,5-Bis(trifluoromethyl)phenyl]-4-[(4-bromo-3-chloro-anilino)methyl]pyrazol-1-yl] benzoic acid (**21**). Light yellow solid; (569 mg, 92%); IR (KBr pellet, cm^{-1}): 3458, 3087, 1704, 1606, 1317, 1278, 1186, 1135; 1H NMR, 300 MHz (DMSO- d_6): δ 8.81 (s, 1H), 8.35 (s, 2H), 8.09–8.05 (m, 5H), 7.37 (d, $J = 5.7$ Hz, 1H), 6.86 (s, 1H), 6.58 (d, $J = 8.4$ Hz, 1H), 4.25 (s, 2H); ^{13}C NMR (75 MHz, DMSO- d_6): δ 167.0, 149.2, 148.8, 142.4, 135.2, 134.0, 133.6, 131.8, 131.4 ($^3J_{C-F} = 3.1$ Hz), 130.8 ($^2J_{C-F} = 32.7$ Hz), 129.1, 127.9, 123.6 ($^1J_{C-F} = 271.2$ Hz), 122.0, 119.9, 118.4, 113.7, 113.5, 106.5, 38.0. HRMS (ESI-FTMS Mass (m/z): calcd for $C_{25}H_{15}BrClF_6N_3O_2$ [$M + H$] $^+$ = 618.0013, 619.9993, found 619.9990.



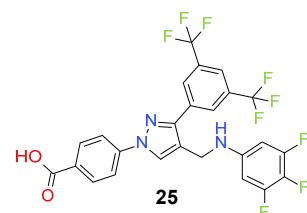
4-[3-[3,5-Bis(trifluoromethyl)phenyl]-4-[[4-fluoro-3-(trifluoromethyl)anilino]methyl]pyrazol-1-yl] benzoic acid (**22**). White solid; (508 mg, 86%); IR (KBr pellet, cm^{-1}): 3429, 3093, 1701, 1608, 1422, 1282, 1154; 1H NMR, 300 MHz (DMSO- d_6): δ 8.83 (s, 1H), 8.37 (s, 2H), 8.06 (s, 5H), 7.22 (br, 1H), 6.93 (s, 2H), 6.44 (s, 1H), 4.30 (s, 2H); ^{13}C NMR (75 MHz, DMSO- d_6): δ 167.0, 152.6 (d, $^1J_{C-F} = 249.0$ Hz), 148.9, 145.4, 142.45, 135.2, 131.8, 131.4 ($^3J_{C-F} = 3.8$ Hz), 130.8 ($^2J_{C-F} = 32.7$ Hz), 128.9 ($^2J_{C-F} = 32.4$ Hz), 127.9, 123.6 ($^1J_{C-F} = 271.1$ Hz), 122.0 ($^3J_{C-F} = 3.6$ Hz), 123.3 ($^1J_{C-F} = 270.1$ Hz), 120.0, 118.4, 117.9 (d, $^2J_{C-F} = 21.1$ Hz), 117.5 (d, $^3J_{C-F} = 7.2$ Hz), 117.0 (dd, $J_{C-F} = 13.5, 24.0$ Hz), 109.4 (d, $^4J_{C-F} = 4.6$ Hz), 38.3. HRMS (ESI-FTMS Mass (m/z): calcd for $C_{26}H_{15}F_{10}N_3O_2$ [$M + H$] $^+$ = 592.1077, found 592.1082.



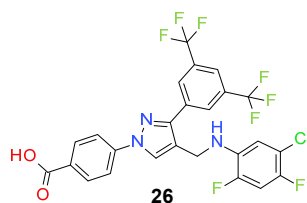
4-[3-[3,5-Bis(trifluoromethyl)phenyl]-4-[[4-bromo-3-(trifluoromethyl)anilino]methyl]pyrazol-1-yl] benzoic acid (**23**). White solid; (543 mg, 83%); IR (KBr pellet, cm^{-1}): 3454, 2983, 1682, 1605, 1439, 1278, 1142; ^1H NMR, 300 MHz (DMSO- d_6): δ 8.83 (s, 1H), 8.36 (s, 2H), 8.11–8.07 (m, 5H), 7.51 (d, $J = 8.7$ Hz, 1H), 7.08 (s, 1H), 6.93–6.81 (m, 2H), 4.35 (s, 2H); ^{13}C NMR (75 MHz, DMSO- d_6): δ 167.0, 148.9, 148.1, 142.4, 135.5 ($^3J_{\text{C-F}} = 29.2$ Hz), 131.4 ($^3J_{\text{C-F}} = 4.8$ Hz), 130.8 ($^2J_{\text{C-F}} = 32.4$ Hz), 129.1, 128.8, 127.9 ($^3J_{\text{C-F}} = 6.1$ Hz), 123.6 ($^1J_{\text{C-F}} = 271.1$ Hz), 122.1, 120.1, 119.8, 118.5, 117.0, 116.2, 111.9, 103.2, 37.9. HRMS (ESI-FTMS Mass (m/z): calcd for $\text{C}_{26}\text{H}_{15}\text{BrF}_9\text{N}_3\text{O}_2$ [$\text{M} + \text{H}$] $^+$ = 652.0277, 654.0258, found 652.0280.



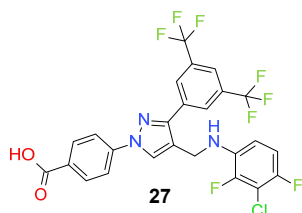
4-[3-[3,5-Bis(trifluoromethyl)phenyl]-4-[(2,3,4-trifluoroanilino)methyl]pyrazol-1-yl] benzoic acid (**24**). White solid; (433 mg, 77%); IR (KBr pellet, cm^{-1}): 3413, 3090, 1694, 1608, 1359, 1281, 1174, 1131; ^1H NMR, 300 MHz (DMSO- d_6): δ 8.74 (s, 1H), 8.39 (s, 2H), 8.12–8.06 (m, 5H), 7.07–7.04 (m, 1H), 6.60–6.58 (m, 1H), 6.17 (s, 1H), 4.39 (s, 2H); ^{13}C NMR (75 MHz, DMSO- d_6): δ 167.0, 148.8, 142.5, 142.3 (dd, $J_{\text{C-F}} = 10.9, 239.0$ Hz), 140.1 (dt, $J_{\text{C-F}} = 7.2, 234.3$ Hz), 139.6 (d, $^1J_{\text{C-F}} = 242.7$ Hz), 135.5, 134.7 (d, $^3J_{\text{C-F}} = 9.6$ Hz), 131.8, 131.4 ($^3J_{\text{C-F}} = 5.0$ Hz), 130.6 ($^2J_{\text{C-F}} = 32.6$ Hz), 129.0, 128.1 (d, $^4J_{\text{C-F}} = 2.7$ Hz), 123.6 ($^1J_{\text{C-F}} = 271.1$ Hz), 121.9, 120.3, 118.4, 111.8 (dd, $J_{\text{C-F}} = 3.2, 18.7$ Hz), 106.6, 38.3. HRMS (ESI-FTMS Mass (m/z): calcd for $\text{C}_{25}\text{H}_{14}\text{F}_9\text{N}_3\text{O}_2$ [$\text{M} + \text{H}$] $^+$ = 560.1015, found 560.1030.



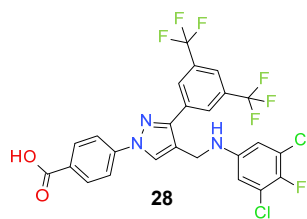
4-[3-[3,5-Bis(trifluoromethyl)phenyl]-4-[(3,4,5-trifluoroanilino)methyl]pyrazol-1-yl] benzoic acid (**25**). White solid; (427 mg, 76%); IR (KBr pellet, cm^{-1}): 3420, 1689, 1608, 1359, 1279, 1178, 1135; ^1H NMR, 300 MHz (DMSO- d_6): δ 8.82 (s, 1H), 8.37 (s, 2H), 8.12–8.08 (m, 5H), 6.54 (s, 3H), 4.29 (s, 2H); ^{13}C NMR (75 MHz, DMSO- d_6): δ 167.0, 152.0 (dt, $J = 10.2, 233.5$ Hz), 148.9, 145.5 (t, $J = 12.1$ Hz), 142.4, 135.2, 132.1 ($^2J_{\text{C-F}} = 38.8$ Hz), 131.5, 130.9 ($^3J_{\text{C-F}} = 8.5$ Hz), 130.5, 129.2, 127.9, 123.6 ($^1J_{\text{C-F}} = 271.1$ Hz), 122.1, 119.7, 118.5, 96.1 (d, $^2J_{\text{C-F}} = 22.9$ Hz), 38.1. HRMS (ESI-FTMS Mass (m/z): calcd for $\text{C}_{25}\text{H}_{14}\text{F}_9\text{N}_3\text{O}_2$ [$\text{M} + \text{H}$] $^+$ = 560.1015, found 560.1026.



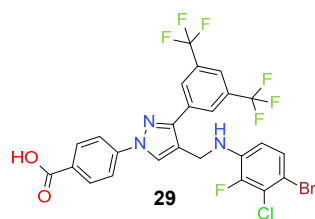
4-[3-[3,5-Bis(trifluoromethyl)phenyl]-4-[(5-chloro-2,4-difluoro-anilino)methyl]pyrazol-1-yl] benzoic acid (**26**). Light yellow solid; (477 mg, 83%); IR (KBr pellet, cm^{-1}): 3446, 3061, 1682, 1608, 1364, 1277, 1175, 1132; ^1H NMR, 300 MHz (DMSO- d_6): δ 8.74 (s, 1H), 8.39 (s, 2H), 8.12–8.06 (m, 5H), 7.37 (t, $J = 9.2$ Hz, 1H), 6.96 (t, $J = 8.3$ Hz, 1H), 6.11 (s, 1H), 4.38 (d, $J = 4.7$ Hz, 2H); ^{13}C NMR (75 MHz, DMSO- d_6): δ 167.0, 149.3 (dd, $J_{\text{C-F}} = 10.3, 246.6$ Hz), 148.9, 148.3 (dd, $J_{\text{C-F}} = 11.3, 240.7$ Hz), 142.5, 135.4, 134.5 (d, $^3J_{\text{C-F}} = 10.7$ Hz), 131.8, 131.4 ($^3J_{\text{C-F}} = 6.7$ Hz), 130.7 ($^2J_{\text{C-F}} = 32.7$ Hz), 129.0, 128.1, 123.6 ($^1J_{\text{C-F}} = 271.1$ Hz), 120.2, 118.4, 115.0 (d, $^2J_{\text{C-F}} = 21.6$ Hz), 112.6 (m), 105.2 (t, $J_{\text{C-F}} = 25.0$ Hz), 79.4 (t, $J_{\text{C-F}} = 32.8$ Hz), 38.2. HRMS (ESI-FTMS Mass (m/z): calcd for $\text{C}_{25}\text{H}_{14}\text{ClF}_8\text{N}_3\text{O}_2$ [$\text{M} + \text{H}$] $^+$ = 576.0720, 578.0692, found 576.0721.



4-[3-[3,5-Bis(trifluoromethyl)phenyl]-4-[(3-chloro-2,4-difluoro-anilino)methyl]pyrazol-1-yl] benzoic acid (**27**). Off white solid; (399 mg, 69%); IR (KBr pellet, cm^{-1}): 3425, 2875, 1694, 1608, 1359, 1278, 1173, 1128; ^1H NMR, 300 MHz (DMSO- d_6): δ 8.74 (s, 1H), 8.39 (s, 2H), 8.12–8.06 (m, 5H), 7.07 (t, $J = 8.9$ Hz, 1H), 6.83–6.78 (m, 1H), 6.11 (s, 1H), 4.41 (s, 2H); ^{13}C NMR (75 MHz, DMSO- d_6): δ 167.0, 149.6 (d, $^1J_{\text{C-F}} = 235.9$ Hz), 148.8, 147.6 (d, $^1J_{\text{C-F}} = 244.6$ Hz), 142.5, 135.5, 134.3 (d, $^3J_{\text{C-F}} = 11.1$ Hz), 131.8, 131.4 ($^3J_{\text{C-F}} = 7.7$ Hz), 130.7 ($^2J_{\text{C-F}} = 25.6$ Hz), 129.0, 128.1, 123.6 ($^1J_{\text{C-F}} = 271.1$ Hz), 122.0, 120.4, 118.4, 111.7 (d, $^2J_{\text{C-F}} = 23.1$ Hz), 111.0 (d, $^4J_{\text{C-F}} = 4.6$ Hz), 108.5 (d, $^2J_{\text{C-F}} = 21.5$ Hz), 38.3. HRMS (ESI-FTMS Mass (m/z): calcd for $\text{C}_{25}\text{H}_{14}\text{ClF}_8\text{N}_3\text{O}_2$ [$\text{M} + \text{H}$] $^+$ = 576.0720, 578.0692, found 576.0729.

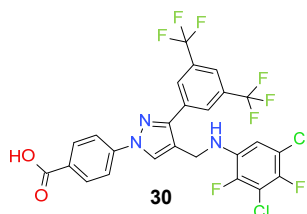


4-[3-[3,5-Bis(trifluoromethyl)phenyl]-4-[(3,5-dichloro-4-fluoro-anilino)methyl]pyrazol-1-yl] benzoic acid (**28**). Light yellow solid; (533 mg, 90%); IR (KBr pellet, cm^{-1}): 3409, 3087, 1686, 1607, 1359, 1282, 1187, 1143; ^1H NMR, 300 MHz (DMSO- d_6): δ 8.81 (s, 1H), 8.36 (s, 2H), 8.12–8.07 (m, 5H), 6.79 (d, $J = 5.6$ Hz, 2H), 6.49 (s, 1H), 4.30 (d, $J = 3.8$ Hz, 2H); ^{13}C NMR (75 MHz, DMSO- d_6): δ 167.0, 148.8, 146.0, 145.3 (d, $^1J_{\text{C-F}} = 233.6$ Hz), 143.8, 135.2, 131.8, 131.4 ($^3J_{\text{C-F}} = 3.2$ Hz), 130.8 ($^2J_{\text{C-F}} = 32.7$ Hz), 129.1 (d, $^3J_{\text{C-F}} = 7.1$ Hz), 127.9, 123.6 ($^1J_{\text{C-F}} = 271.2$ Hz), 122.0, 121.5 (d, $^2J_{\text{C-F}} = 17.7$ Hz), 119.8, 118.4, 118.2, 112.1, 79.4 (t, $J_{\text{C-F}} = 33.0$ Hz), 38.1. HRMS (ESI-FTMS Mass (m/z): calcd for $\text{C}_{25}\text{H}_{14}\text{Cl}_2\text{F}_7\text{N}_3\text{O}_2$ [$\text{M} + \text{H}$] $^+$ = 592.0424, 594.0396, found 592.0402.



4-[3-[3,5-Bis(trifluoromethyl)phenyl]-4-[(4-bromo-3-chloro-2-fluoro-anilino)methyl]pyrazol-1-yl] benzoic acid (**29**). Light yellow solid; (558 mg, 88%); IR (KBr pellet, cm^{-1}): 3464, 2860,

1686, 1601, 1424, 1064; ^1H NMR, 300 MHz (DMSO- d_6): δ 8.72 (s, 1H), 8.37 (s, 2H), 8.14–8.07 (m, 5H), 7.32 (d, $J = 8.8$ Hz, 1H), 6.75 (t, $J = 8.5$ Hz, 1H), 6.49 (s, 1H), 4.44 (d, $J = 4.5$ Hz, 2H); ^{13}C NMR (75 MHz, DMSO- d_6): δ 167.0, 148.7, 147.4 (d, $^1J_{\text{C-F}} = 243.0$ Hz), 142.5, 137.2 (d, $^3J_{\text{C-F}} = 12.0$ Hz), 135.5, 131.4, 130.6 ($^2J_{\text{C-F}} = 33.2$ Hz), 129.0, 128.7 ($^3J_{\text{C-F}} = 3.0$ Hz), 128.1, 123.6 ($^1J_{\text{C-F}} = 271.1$ Hz), 122.0, 120.4 (d, $^2J_{\text{C-F}} = 24.6$ Hz), 118.4, 117.1, 112.6, 106.8, 103.2 (t, $J_{\text{C-F}} = 20.9$ Hz), 38.1. HRMS (ESI-FTMS Mass (m/z): calcd for $\text{C}_{25}\text{H}_{14}\text{BrClF}_7\text{N}_3\text{O}_2$ [$\text{M} + \text{H}$] $^+$ = 635.9919, 637.9899, found 637.9897.



4-[3-[3,5-Bis(trifluoromethyl)phenyl]-4-[(3,5-dichloro-2,4-difluoro-anilino)methyl]pyrazol-1-yl]benzoic acid (**30**). Off white solid; (413 mg, 67%); IR (KBr pellet, cm^{-1}): 3427, 3088, 1694, 1608, 1360, 1278, 1178, 1135; ^1H NMR, 300 MHz (DMSO- d_6): δ 8.72 (s, 1H), 8.36 (s, 2H), 8.12–8.06 (m, 5H), 6.99 (t, $J = 7.6$ Hz, 1H), 6.45 (d, $J = 4.32$ Hz, 1H), 4.45 (s, 2H); ^{13}C NMR (75 MHz, DMSO- d_6): δ 167.0, 148.8, 145.8 (d, $^1J_{\text{C-F}} = 243.7$ Hz), 144.9 (d, $^1J_{\text{C-F}} = 235.9$ Hz), 142.5, 135.5, 134.6 (dd, $J_{\text{C-F}} = 7.5, 10.0$ Hz), 131.8, 131.4 (d, $^3J_{\text{C-F}} = 6.1$ Hz), 130.6 ($^2J_{\text{C-F}} = 36.8$ Hz), 129.0, 128.1, 123.6 ($^1J_{\text{C-F}} = 271.4$ Hz), 122.0, 120.2, 118.5, 116.2 (d, $^2J_{\text{C-F}} = 19.1$ Hz), 110.7 ($^3J_{\text{C-F}} = 3.7$ Hz), 109.8 (t, $J_{\text{C-F}} = 19.7$ Hz), 38.0. HRMS (ESI-FTMS Mass (m/z): calcd for $\text{C}_{25}\text{H}_{13}\text{Cl}_2\text{F}_8\text{N}_3\text{O}_2$ [$\text{M} + \text{H}$] $^+$ = 610.0330, 612.0302, found 610.0322.

3.5. Minimum Inhibitory Concentration Assay (MIC)

As previously reported, the MIC values of the substances were calculated using the standard microdilution technique suggested by the Clinical and Laboratory Standards Institute (CLSI) [36]. Compounds were dissolved in dimethyl sulfoxide (DMSO) to achieve a starting concentration of 32 $\mu\text{g}/\text{mL}$ as described by us previously [29,31]. Compounds were further diluted two-fold across the 96-well honeycomb plate columns in cation adjusted Mueller Hinton broth (CAMHB), and bacterial culture was added. Plates were incubated for 18–20 h at 35 $^\circ\text{C}$ before determining the minimum concentrations at which wells had no visible turbidity to the naked eye. The MIC values were determined from at least a duplicate result obtained from three independent experiments using fresh bacterial cultures on different days.

3.6. Cytotoxicity Assay

The human embryonic kidney cell line (HEK-293) was used to assess the cytotoxicity of the antibiotics as described by us previously [29,31]. HEK-293 cells were cultured in Dulbecco's modified eagle's medium (DMEM) containing 10% Fetal Bovine Serum (FBS) and incubated at 37 $^\circ\text{C}$ in the presence of 5% carbon dioxide. HEK-293 cells were cultured in 96-well black plates with 6000 cells per well for the first 24 h followed by treatment with a range of concentrations of antibiotics dissolved in DMSO for the next 24 h. After the second period of incubation, resazurin (40 μL of 0.15 mg/mL) was added to each well and incubated for an additional 4 h. Reduction of resazurin was measured fluorometrically with excitation wavelength at 560 nm and emission at 590 nm using BioTek™ Cytation™ 5 plate reader. Percentage viability of HEK cells for each range of concentrations was calculated, taking the fluorescence value of the wells treated with DMSO as a reference, using Microsoft® Excel® for Office 365 MSO. IC_{50} values were computed using the calculated percentage viability values through data processing in Graphpad Prism 7 for Windows, Version 7.04.

3.7. Time Kill Assay

Time Kill Assay was performed against *S. aureus* ATCC 33599 using our potent compounds following methodology reported previously with few modifications [29,31]. The bacterial strain was grown to its logarithmic growth phase by shaking at 200 rpm in a shaking incubator at 35 °C. The culture was diluted to $\sim 1.5 \times 10^7$ CFU/mL in CAMHB and treated with concentrations equivalent to $4 \times$ MIC of tested compounds, including vancomycin and daptomycin, as control drugs. Aliquots were collected from treatment every two hours of incubation at 35 °C up to 12 h and one in 24 h, then serially diluted in sterile $1 \times$ PBS. The diluted aliquots were then transferred to blood agar plates by using the 6×6 drop plate method and incubated at 35 °C for 18–20 h prior to colony counting to obtain CFU/mL. Time-kill line graphs (CFU/mL vs. time) were constructed using Microsoft® Excel® for Office 365 MSO.

3.8. Persister Assay

The persister assay was performed following the methodology described previously [29]. Briefly, for persister viability assays, *S. aureus* ATCC 700699 strain (MRSA) was grown to stationary phase in CAMHB medium by shaking at 200 rpm in a shaking incubator for 24 h at 35 °C. An aliquot of stationary phase culture was washed and diluted to $\sim 5 \times 10^8$ CFU/mL in $1 \times$ PBS then treated with $32 \times$ MIC of each compound and control drugs in sterile 10×75 mm plastic culture tubes and incubated at 35 °C with shaking at 200 rpm for 4 h. After incubation, 400 μ L aliquot was washed, serially diluted in PBS, and plated in blood agar plate for viable colony count.

Likewise, for persister time-kill assays, the persister cells were treated at varied concentrations and incubated with shaking. At the start and every 2 h until 8 h, 400 μ L samples were washed, serially diluted, and plated on blood agar using the 6×6 drop plate method. Plates were incubated for 18–20 h at 35 °C, before the colonies were counted to calculate CFU/mL. All the treatments were performed in triplicates.

3.9. Calgary Biofilm Device

Minimum biofilm eradication concentration (MBEC) was determined using a Calgary device using the protocol reported elsewhere with some modifications [37]. The Calgary device is a 96-well plate with a lid containing pegs to establish biofilms. Bacteria from an overnight plate culture were suspended to a 0.5 McFarland turbidity, then diluted 1:100 in a CAMHB containing 1% glucose which was inoculated in the 96 wells (150 μ L in each well) and incubated at 35 °C for 24 h to establish biofilm on the pegs. The lid was then removed, washed with PBS in a fresh 96 well plate, then transferred to another 96-well plate containing 2-fold serial dilutions of the test compounds dissolved in PBS (150 μ L total volume in each well). This plate was called the “challenge plate”. The challenge plate was incubated for an additional 24 h, and the lid was transferred to the next 96-well plate containing fresh CAMHB media with 1% glucose (180 μ L) and further incubated for 24 h. After this final incubation, the wells were observed for visible turbidity. MBEC was the well with the lowest concentration of compound that resulted in no turbidity. All the compounds were tested in a minimum of three independent experiments.

4. Conclusions

In summary, we are reporting an efficient synthesis of 30 novel pyrazole derivatives. Most of these compounds are potent growth inhibitors of Gram-positive bacterial strains with MIC values as low as 0.25 μ g/mL. These bactericidal compounds are potent against MRSA persisters. Three of the four compounds tested for their biofilm eradication property showed potent activity. Enthusiasm was a little bit dampened, due to the toxicity of the compounds for human cell lines. Nevertheless, these potent compounds can be modified to increase their pharmacological properties and reduce their toxicity profile.

Supplementary Materials: Figure S1–S31: Characterization data (I–B).

Author Contributions: I.S.A., H.R.K., M.K.A.-g., and S.R.—methodology, investigation, and validation; M.A.A.—conceptualization, project administration, manuscript writing—original draft and supervision; D.F.G.—supervision and manuscript editing. All authors have read and agreed to the published version of the manuscript.

Funding: This research was funded by Arkansas INBRE P20 GM103429 and the Kays Foundation grant. ABI provided different resources to accomplish the project.

Institutional Review Board Statement: Not applicable.

Informed Consent Statement: Not applicable.

Data Availability Statement: Not applicable.

Acknowledgments: This manuscript was made possible by the Arkansas INBRE Summer Research Grant, supported by a grant from the National Institute of General Medical Sciences, (NIGMS), P20 GM103429, from the National Institutes of Health. The Research Technology Core of the Arkansas INBRE program, supported by a grant from the National Institute of General Medical Sciences, (NIGMS), P20 GM103429, from the National Institutes of Health, was helpful to get HRMS data. The Kays Foundation grant was the key to completing antimicrobial studies. We are thankful to the Department of Chemistry and Physics, and Arkansas Biosciences Institute at the Arkansas State University for providing infrastructure and support.

Conflicts of Interest: The authors declare no conflict of interest.

Sample Availability: Samples of the compounds (1–30) are available from the authors.

References

1. Oliveira, D.M.P.D.; Forde, B.M.; Kidd, T.J.; Harris, P.N.A.; Schembri, M.A.; Beatson, S.A.; Paterson, D.L.; Walker, M.J. Antimicrobial Resistance in ESKAPE Pathogens. *Clin. Microbiol. Rev.* **2020**, *33*, e00181-19. [CrossRef] [PubMed]
2. Agudelo Higuera, N.I.; Huycke, M.M. Enterococcal Disease, Epidemiology, and Implications for Treatment. In *Enterococci: From Commensals to Leading Causes of Drug Resistant Infection*; Gilmore, M.S., Clewell, D.B., Ike, Y., Shankar, N., Eds.; Massachusetts Eye and Ear Infirmary: Boston, MA, USA, 2014.
3. CDC Vancomycin-Resistant Enterococci (VRE). Available online: <https://www.cdc.gov/drugresistance/pdf/threats-report/vre-508.pdf> (accessed on 23 May 2020).
4. Ch'ng, J.-H.; Chong, K.K.L.; Lam, L.N.; Wong, J.J.; Kline, K.A. Biofilm-Associated Infection by Enterococci. *Nat. Rev. Microbiol.* **2019**, *17*, 82–94. [CrossRef] [PubMed]
5. Pidot, S.J.; Gao, W.; Buultjens, A.H.; Monk, I.R.; Guerillot, R.; Carter, G.P.; Lee, J.Y.H.; Lam, M.M.C.; Grayson, M.L.; Ballard, S.A.; et al. Increasing Tolerance of Hospital Enterococcus Faecium to Handwash Alcohols. *Sci. Transl. Med.* **2018**, *10*, eaar6115. [CrossRef]
6. CDC General Information about Staphylococcus Aureus. Available online: <https://www.cdc.gov/hai/organisms/staph.html> (accessed on 15 July 2021).
7. Craft, K.M.; Nguyen, J.M.; Berg, L.J.; Townsend, S.D. Methicillin-Resistant Staphylococcus Aureus (MRSA): Antibiotic-Resistance and the Biofilm Phenotype. *Medchemcomm* **2019**, *10*, 1231–1241. [CrossRef]
8. Mistry, T.L.; Truong, L.; Ghosh, A.K.; Johnson, M.E.; Mehboob, S. Benzimidazole-Based FabI Inhibitors: A Promising Novel Scaffold for Anti-staphylococcal Drug Development. *ACS Infect. Dis.* **2017**, *3*, 54–61. [CrossRef]
9. Moisse, K. Antibiotic Resistance Could Bring 'End of Modern Medicine'. Available online: <http://abcnews.go.com/blogs/health/2012/03/16/antibiotic-resistance-could-bring-end-of-modern-medicine/> (accessed on 1 May 2020).
10. Naim, M.J.; Alam, O.; Nawaz, F.; Alam, M.J.; Alam, P. Current Status of Pyrazole and Its Biological Activities. *J. Pharm. Bioallied. Sci.* **2016**, *8*, 2–17.
11. Steinbach, G.; Lynch, P.M.; Phillips, R.K.S.; Wallace, M.H.; Hawk, E.; Gordon, G.B.; Wakabayashi, N.; Saunders, B.; Shen, Y.; Fujimura, T.; et al. The Effect of Celecoxib, a Cyclooxygenase-2 Inhibitor, in Familial Adenomatous Polyposis. *N. Engl. J. Med.* **2000**, *342*, 1946–1952. [CrossRef]
12. Hampp, C.; Hartzema, A.G.; Kauf, T.L. Cost-Utility Analysis of Rimonabant in the Treatment of Obesity. *Value Health* **2008**, *11*, 389–399. [CrossRef] [PubMed]
13. Kameyama, T.; Nabeshima, T. Effects of 1,3-Diphenyl-5-(2-Dimethylaminopropionamide)-Pyrazole[Difenamizole] on a Conditioned Avoidance-Response. *Neuropharmacology* **1978**, *17*, 249–256. [PubMed]
14. Dalvie, D.K.; Kalgutkar, A.S.; Khojasteh-Bakht, S.C.; Obach, R.S.; O'Donnell, J.P. Biotransformation Reactions of Five-Membered Aromatic Heterocyclic Rings. *Chem. Res. Toxicol.* **2002**, *15*, 269–299. [CrossRef] [PubMed]
15. Chen, L.W.; Wang, P.F.; Tang, D.J.; Tao, X.X.; Man, R.J.; Qiu, H.Y.; Wang, Z.C.; Xu, C.; Zhu, H.L. Metronidazole Containing Pyrazole Derivatives Potently Inhibit Tyrosyl-tRNA Synthetase: Design, Synthesis, and Biological Evaluation. *Chem. Biol. Drug. Des.* **2016**, *88*, 592–598. [CrossRef]

16. Hafez, H.N.; El-Gazzar, A.R.; Al-Hussain, S.A. Novel Pyrazole Derivatives with Oxa/Thiadiazolyl, Pyrazolyl Moieties and Pyrazolo [4,3-d]-Pyrimidine Derivatives as Potential Antimicrobial and Anticancer Agents. *Bioorg. Med. Chem. Lett.* **2016**, *26*, 2428–2433. [CrossRef] [PubMed]
17. Nayak, N.; Ramprasad, J.; Dalimba, U. New INH-Pyrazole Analogs: Design, Synthesis and Evaluation of Antitubercular and Antibacterial Activity. *Bioorg. Med. Chem. Lett.* **2015**, *25*, 5540–5545. [CrossRef]
18. Allison, D.; Delancey, E.; Ramey, H.; Williams, C.; Alsharif, Z.A.; Al-khattabi, H.; Ontko, A.; Gilmore, D.; Alam, M.A. Synthesis and Antimicrobial Studies of Novel Derivatives of 4-(4-formyl-3-phenyl-1H-pyrazol-1-yl)Benzoic Acid as Potent Anti-Acinetobacter Baumannii Agents. *Bioorg. Med. Chem. Lett.* **2017**, *27*, 387–392. [CrossRef] [PubMed]
19. Zakeyah, A.A.; Whitt, J.; Duke, C.; Gilmore, D.F.; Meeker, D.G.; Smeltzer, M.S.; Alam, M.A. Synthesis and Antimicrobial Studies of Hydrazone Derivatives of 4-[3-(2,4-Difluorophenyl)-4-formyl-1H-pyrazol-1-yl]benzoic acid and 4-[3-(3,4-difluorophenyl)-4-formyl-1H-Pyrazol-1-yl]Benzoic Acid. *Bioorg. Med. Chem. Lett.* **2018**, *28*, 2914–2919. [CrossRef] [PubMed]
20. Whitt, J.; Duke, C.; Sumlin, A.; Chambers, S.A.; Alnufaie, R.; Gilmore, D.; Fite, T.; Basnakian, A.G.; Alam, M.A. Synthesis of Hydrazone Derivatives of 4-[4-Formyl-3-(2-oxochromen-3-yl)pyrazol-1-yl]Benzoic acid as Potent Growth Inhibitors of Antibiotic-Resistant Staphylococcus Aureus and Acinetobacter Baumannii. *Molecules* **2019**, *24*, 2051. [CrossRef]
21. Brider, J.; Rowe, T.; Gibler, D.J.; Gottsponer, A.; Delancey, E.; Branscum, M.D.; Ontko, A.; Gilmore, D.; Alam, M.A. Synthesis and antimicrobial studies of azomethine and N-arylamine derivatives of 4-(4-formyl-3-phenyl-1H-pyrazol-1-yl)Benzoic Acid as Potent Anti-Methicillin-Resistant Staphylococcus Aureus Agents. *Med. Chem. Res.* **2016**, *25*, 2691–2697. [CrossRef]
22. Whitt, J.; Duke, C.; Ali, M.A.; Chambers, S.A.; Khan, M.M.K.; Gilmore, D.; Alam, M.A. Synthesis and Antimicrobial Studies of 4-[3-(3-Fluorophenyl)-4-formyl-1H-Pyrazol-1-yl]Benzoic Acid and 4-[3-(4-Fluorophenyl)-4-formyl-1H-pyrazol-1-yl]benzoic Acid as Potent Growth Inhibitors of Drug-Resistant Bacteria. *ACS Omega* **2019**, *4*, 14284–14293. [CrossRef]
23. Ahn, M.; Gunasekaran, P.; Rajasekaran, G.; Kim, E.Y.; Lee, S.-J.; Bang, G.; Cho, K.; Hyun, J.-K.; Lee, H.-J.; Jeon, Y.H.; et al. Pyrazole Derived Ultra-Short Antimicrobial Peptidomimetics with Potent Anti-Biofilm Activity. *Eur. J. Med. Chem.* **2017**, *125*, 551–564. [CrossRef]
24. Khan, M.F.; Alam, M.M.; Verma, G.; Akhtar, W.; Akhter, M.; Shaquiquzzaman, M. The Therapeutic Voyage of Pyrazole and its Analogs: A Review. *Eur. J. Med. Chem.* **2016**, *120*, 170–201. [CrossRef]
25. Sidhartha, S.K.; Cinu, A.T. Strategically Placed Trifluoromethyl Substituent in the Realm of Antitubercular Drug Design. *Curr. Drug Ther.* **2019**, *14*, 114–123.
26. Keam, S.J.; Scott, L.J. Dutasteride: A Review of its Use in the Management of Prostate Disorders. *Drugs* **2008**, *68*, 463–485. [CrossRef]
27. Shang, Z.; Li, Y.; Zhang, M.; Tian, J.; Han, R.; Shyr, C.R.; Messing, E.; Yeh, S.; Niu, Y.; Chang, C. Antiandrogen Therapy with Hydroxyflutamide or Androgen Receptor Degradation Enhancer ASC-J9 Enhances BCG Efficacy to Better Suppress Bladder Cancer Progression. *Mol. Cancer Ther.* **2015**, *14*, 2586–2594. [CrossRef] [PubMed]
28. Junaid, Z.; Patel, J. *Cinacalcet*; StatPearls: Treasure Island, FL, USA, 2021.
29. Hansa, R.K.C.; Khan, M.M.K.; Frangie, M.M.; Gilmore, D.F.; Shelton, R.S.; Savenka, A.V.; Basnakian, A.G.; Shuttleworth, S.L.; Smeltzer, M.S.; Alam, M.A. 4-(4-(Anilinomethyl)-3-[4-(trifluoromethyl)phenyl]-1H-Pyrazol-1-yl)benzoic Acid Derivatives as Potent Anti-Gram-Positive Bacterial Agents. *Eur. J. Med. Chem.* **2021**, *219*, 113402. [CrossRef]
30. Alnufaie, R.; Kc, H.R.; Alsup, N.; Whitt, J.; Chambers, S.A.; Gilmore, D.; Alam, M.A. Synthesis and Antimicrobial Studies of Coumarin-Substituted Pyrazole Derivatives as Potent Anti-Staphylococcus Aureus Agents. *Molecules* **2020**, *25*, 2758. [CrossRef]
31. Alnufaie, R.; Alsup, N.; Kc, H.R.; Newman, M.; Whitt, J.; Chambers, S.A.; Gilmore, D.; Alam, M.A. Design and Synthesis of 4-[4-formyl-3-(2-naphthyl)pyrazol-1-yl]benzoic Acid Derivatives as Potent Growth Inhibitors of Drug-Resistant Staphylococcus aureus. *J. Antibiot.* **2020**, *73*, 818–827. [CrossRef]
32. Delancey, E.; Allison, D.; KC, H.R.; Gilmore, D.F.; Fite, T.; Basnakian, A.G.; Alam, M.A. Synthesis of 4,4-(4-Formyl-1H-pyrazole-1,3-diyl)dibenzoic Acid Derivatives as Narrow Spectrum Antibiotics for the Potential Treatment of Acinetobacter Baumannii Infections. *Antibiotics* **2020**, *9*, 650. [CrossRef]
33. Scheper, H.; Wubbolts, J.M.; Verhagen, J.A.M.; de Visser, A.W.; van der Wal, R.J.P.; Visser, L.G.; de Boer, M.G.J.; Nibbering, P.H. SAAP-148 Eradicates MRSA Persists Within Mature Biofilm Models Simulating Prosthetic Joint Infection. *Front. Microbiol.* **2021**, *12*, 625952. [CrossRef] [PubMed]
34. Kim, W.; Zou, G.; Hari, T.P.A.; Wilt, I.K.; Zhu, W.; Galle, N.; Faizi, H.A.; Hendricks, G.L.; Tori, K.; Pan, W.; et al. A Selective Membrane-Targeting Repurposed Antibiotic with Activity against Persistent Methicillin-resistant staphylococcus Aureus. *Proc. Natl. Acad. Sci. USA* **2019**, *116*, 16529–16534. [CrossRef]
35. Kim, W.; Zhu, W.; Hendricks, G.L.; Van Tyne, D.; Steele, A.D.; Keohane, C.E.; Fricke, N.; Conery, A.L.; Shen, S.; Pan, W.; et al. A New Class of Synthetic Retinoid Antibiotics Effective against Bacterial Persisters. *Nature* **2018**, *556*, 103–107. [CrossRef]
36. Methods for Dilution Antimicrobial Susceptibility Tests for Bacteria that Grow Aerobically. CLSI Approved Standards M7-A11. Clinical and Laboratory Standards Institute, Wayne, 2018. Available online: https://clsi.org/media/1928/m07ed11_sample.pdf (accessed on 26 March 2020).
37. Garrison, A.T.; Abouelhassan, Y.; Kallifidas, D.; Tan, H.; Kim, Y.S.; Jin, S.; Luesch, H.; Huigens, R.W. An Efficient Buchwald–Hartwig/Reductive Cyclization for the Scaffold Diversification of Halogenated Phenazines: Potent Antibacterial Targeting, Biofilm Eradication, and Prodrug Exploration. *J. Med. Chem.* **2018**, *61*, 3962–3983. [CrossRef] [PubMed]